Proteome Analysis of Cytoplasmatic and Plastidic β-Carotene Lipid Droplets in *Dunaliella bardawil*[1][OPEN]

Lital Davidi, Yishai Levin, Shifra Ben-Dor, and Uri Pick*

Department of Biological Chemistry (L.D., U.P.), Nancy and Stephen Grand Israel National Center for Personalized Medicine (Y.L.), and Biological Services Unit (S.B.-D.), Weizmann Institute of Science, Rehovot 76100, Israel

The halotolerant green alga *Dunaliella bardawil* is unique in that it accumulates under stress two types of lipid droplets: cytoplasmatic lipid droplets (CLD) and β-carotene-rich (βC) plastoglobuli. Recently, we isolated and analyzed the lipid and pigment compositions of these lipid droplets. Here, we describe their proteome analysis. A contamination filter and an enrichment filter were utilized to define core proteins. A proteome database of *Dunaliella salina/D. bardawil* was constructed to aid the identification of lipid droplet proteins. A total of 124 and 42 core proteins were identified in βC-plastoglobuli and CLD, respectively, with only eight common proteins. *Dunaliella* spp. CLD resemble cytoplasmic droplets from *Chlamydomonas reinhardtii* and contain major lipid droplet-associated protein and enzymes involved in lipid and sterol metabolism. The βC-plastoglobuli proteome resembles the *C. reinhardtii* eyespot and Arabidopsis (*Arabidopsis thaliana*) plastoglobule proteomes and contains carotene-globule-associated protein, plastid-lipid-associated protein-fibrillins, SOUL heme-binding proteins, phytyl ester synthases, β-carotene biosynthesis enzymes, and proteins involved in membrane remodeling/lipid droplet biogenesis: VESICLE-INDUCING PLASTID PROTEIN1, synaptotagmin, and the eyespot assembly proteins EYE3 and SOUL3. Based on these and previous results, we propose models for the biogenesis of βC-plastoglobuli and the biosynthesis of β-carotene within βC-plastoglobuli and hypothesize that βC-plastoglobuli evolved from eyespot lipid droplets.

Lipid droplets are the least characterized organelles in both mammalian and plant cells, and they were considered until a few years ago as passive storage compartments for triglycerides (TAG), sterol esters, and some pigments. However, recent studies have shown that they have diverse metabolic functions (Goodman, 2008; Farese and Walther, 2009; Murphy, 2012). Proteomic analyses in plants and some microalgae have shown that lipid droplets in the cytoplasm and in the chloroplast contain a large diversity of proteins including both structural proteins and many enzymes, indicating that they take an active metabolic role in the synthesis, degradation, and mobilization of glycerolipids, sterols, and pigments as well as in regulatory functions that have not yet been clarified (Schmidt et al., 2006; Ytterberg et al., 2006; Nguyen et al., 2011; Lundquist et al., 2012b; Eugeni Piller et al., 2014). A major limitation for determining the proteomes of lipid droplets, particularly in microalgae, is the purity and the homogeneity of the preparation. Green microalgae, for example, may contain three distinct pools of lipid droplets in one cell: the cytoplasmatic lipid droplets (CLD), the major neutral lipid pool, which are induced under stress conditions such as nitrogen limitation or at the stationary growth phase (Wang et al., 2009); plastoglobules, which are smaller lipid droplets within the chloroplast that have been shown to change in size and number under stress conditions and seem to be involved in stress resistance, metabolite transport, and the regulation of photosynthetic electron transport (Bréhélin et al., 2007; Besagni and Kessler, 2013); and the eyespot structure, part of the visual system in green algae, composed of one or several layers of lipid droplets, characterized by their orange color resulting from a high content of β-carotene (Kreimer, 2009). Disruption of microalgal cells, which is required for the isolation of the lipid droplets, usually involves harsh treatments such as sonication, mixing with glass beads, or use of a French press that breaks not only the cell membrane but also the chloroplast. Therefore, it is almost impossible to separate the different lipid droplet classes by the subsequent density gradient centrifugation, making it difficult to assign the origin of identified proteins. The other major difficulty is contamination by proteins released during cell lysis and fractionation, which associate and copurify with lipid droplets. These include cytoplasmic, chloroplastic, and mitochondrial proteins (Moellering and Benning, 2010; James et al., 2011; Nguyen et al., 2011; Nojima et al., 2013). Purification of isolated lipid droplets from loosely associated proteins is possible by treatments with detergents, high salt, and chaotropic agents (Jolivet et al., 2004; Nguyen et al., 2011); however, the danger in such treatments is that they also remove native loosely associated proteins from the lipid droplets.

[1] This work was supported by the Ruth and Herman Albert Scholars Program for New Scientists (to Y.L.), the Charles and Louise Gartner Fund, and the Alternative Energy Research Initiative Center at the Weizmann Institute (to U.P.).

* Address correspondence to uri.pick@weizmann.ac.il.

The author responsible for distribution of materials integral to the findings presented in this article in accordance with the policy described in the Instructions for Authors (www.plantphysiol.org) is: Uri Pick (uri.pick@weizmann.ac.il).

[OPEN] Articles can be viewed without a subscription.

www.plantphysiol.org/cgi/doi/10.1104/pp.114.248450

 © 2014 American Society of Plant Biologists. All Rights Reserved.

In this work, we tried to circumvent these problems by choosing a special algal species that is suitable for controlled cell lysis and fractionation and by utilizing two different contamination filters.

The alga we selected, *Dunaliella bardawil*, is unique in that it accumulates large amounts of two different types of lipid droplets, CLD and β-carotene-rich (βC) plastoglobuli, under stress conditions (Davidi et al., 2014). The lack of a rigid cell wall in this alga allows lysis of the plasma membrane by a gentle osmotic shock, releasing CLD but leaving the chloroplast intact (Katz et al., 1995). This enables the recovery of large quantities of the two types of highly purified lipid droplets by differential lysis. In a recent study, we described the isolation and lipid compositions of these two lipid pools and showed that they have similar TAG compositions but different lipid-associated major proteins (Davidi et al., 2014).

The high nutritional and pharmacological value of β-carotene for humans has promoted intensive research aimed to clarify its biosynthesis and regulation in plants and also led to attempts to increase β-carotene levels by genetic manipulations in crop plants such as tomato (*Solanum lycopersicum*; Rosati et al., 2000; Giorio et al., 2007) or by the creation of Golden rice (*Oryza sativa*; Ye et al., 2000). However, the capacity of plants to store β-carotene is limited, and in this respect, *D. bardawil* is an exceptional example of an organism that can accumulate large amounts of this pigment, up to 10% of its dry weight. This is enabled by the compartmentation and storage of this lipophilic pigment in specialized plastoglobules. Also, the unusual isomeric composition, consisting of around 50% 9-cis- and 50% all-trans-isomers (Ben-Amotz et al., 1982, 1988), is probably of major importance in this respect, due to the better solubility of the cis-isomer in lipids, which enables the storage of high concentrations exceeding 50% of the lipid droplets. The localization of carotenoid biosynthesis in plants appears to be tissue specific: in green tissues, it takes place in chloroplast membranes, probably within the inner chloroplast envelope membrane (Joyard et al., 2009), whereas in carotenoid-accumulating fruits, such as tomato or bell pepper (*Capsicum annuum*), it takes place in specialized organelles derived from chromoplasts (Siddique et al., 2006; Barsan et al., 2010). In green microalgae, there are at least two types of carotenoid-accumulating organelles: CLD and eyespot. Algae such as *Haematococcus pluvialis* and *Chlorella zofigiensis* accumulate carotenoids within CLD. In *H. pluvialis*, the major pigment, astaxanthin, is synthesized initially in the chloroplast as β-carotene and then transferred to CLD, where it is oxidized and hydroxylated to astaxanthin (Grünewald et al., 2001). The eyespot, which is composed of one or several layers of small β-carotene-containing lipid droplets, has been shown by proteomic analysis to include part of the β-carotene biosynthesis enzymes, indicating that β-carotene is probably synthesized within these lipid droplets (Schmidt et al., 2006). Similarly, plant chromoplasts also contain carotenoid biosynthesis enzymes (Schmidt et al., 2006; Ytterberg et al., 2006; Schapire et al., 2009). *D. bardawil* and *Dunaliella salina* are unique in that they accumulate large amounts of

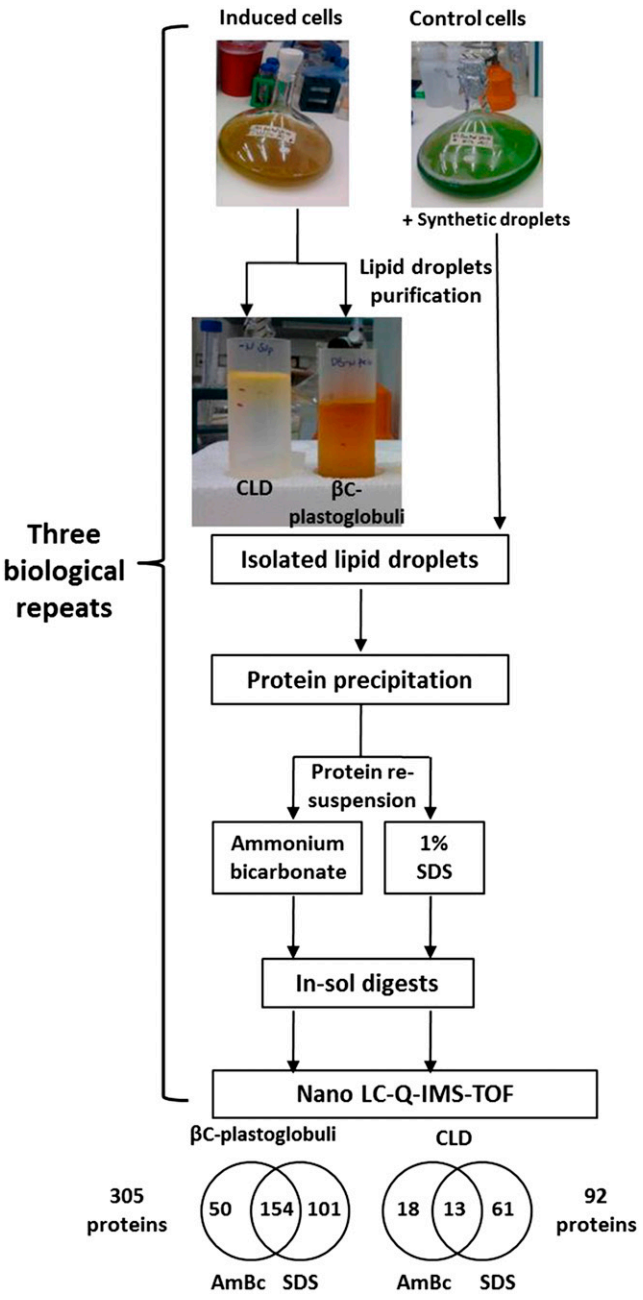

Figure 1. Scheme of the isolation and identification of the CLD and βC-plastoglobuli proteomes. Lipid droplets were prepared from *D. bardawil* cells cultured without nitrogen for 2 d and from nitrogen-sufficient cells supplemented with synthetic globules. Thylakoids were isolated from nitrogen-sufficient cells. Proteins were precipitated in acetone and resuspend first in 50 mM AmBc and next in 1% SDS. Each sample was digested with trypsin. Peptide digests were analyzed by nanoliquid chromatography quadrupole ion mobility time-of-flight mass spectrometry (LC-Q-IMS-TOF). A total of 570 proteins were identified in both lipid pools. Proteins with at least two peptides in at least two biological repeats were analyzed. A total of 305 and 92 unique proteins were identified in βC-plastoglobuli and CLD, respectively, 154 and 13 of which were identified by both experimental methods in βC-plastoglobuli and CLD, respectively. In-sol, In solution.

β-carotene within βC-plastoglobuli. A special focus in this work was the identification of the β-carotene biosynthesis machinery in *D. bardawil*. It is not known if the synthesis takes place inside the lipid βC-plastoglobuli or in chloroplast envelope membranes. Since *D. bardawil* also contains β-carotene and xanthophylls at the photosynthetic system, it is interesting to know whether the β-carotene that accumulates under stress in βC-plastoglobuli is produced by the constitutive carotenoid biosynthetic pathway or by a different stress-induced enzymatic system.

RESULTS AND DISCUSSION

Protein Extraction

In this work, we introduced two filters for contamination to analyze the proteomes of these lipid droplets: one involves the addition of synthetic lipid dispersion to control cells during cell fractionation (Davidi et al., 2012). The rationale for this filter was that contaminating proteins released from other organelles could be identified in the isolated synthetic lipid droplets (contamination filter). We also determined the proteome of an isolated thylakoid membrane preparation and compared the enrichment of the protein of lipid droplets relative to the thylakoid membrane proteins (enrichment filter; Lundquist et al., 2012b).

Isolation of two types of lipid droplets from *D. bardawil* was performed as described in our recent article (Davidi et al., 2014). In brief, cells deprived from nitrogen for 2 d were lysed by an osmotic shock and separated to CLD and chloroplasts. Chloroplasts were washed and lysed by sonication to release the βC-plastoglobuli. Three independent preparations of CLD and βC-plastoglobuli (two samples of each, a total of six repeats) were purified by Suc density gradient centrifugation. The purity of the two preparations was verified by the absence of chlorophyll, by negative western analysis tests for chloroplast major proteins, and by the lack of cross-contaminations by the different major lipid-associated proteins or by β-carotene (Davidi et al., 2014). Proteins were precipitated in 80% (v/v) acetone at −20°C and suspended and extracted in 50 mM ammonium bicarbonate (AmBc), and the insoluble pellet was reextracted with 1% SDS. For thylakoid proteins, chloroplast membranes of noninduced cells were washed several times, lipids were extracted by acetone precipitation, and the pellet was extracted with SDS as above. All protein extracts were digested with trypsin. The samples containing SDS were cleaned using detergent-removal columns (Pierce). The digested peptides were analyzed by nanoliquid chromatography-tandem mass spectrometry. Semiquantitative comparisons were conducted by spectral counting.

In order to analyze the lipid droplet proteomes, we constructed a proteome database of *D. salina* CCAP 19/18/*D. bardawil*, which was based on protein, EST, and complementary DNA (cDNA) sequences available at the National Center for Biotechnology Information (NCBI) and from the Joint Genome Institute (JGI) *D. salina* sequencing program (provided by Jon Magnuson, John Cushman, and Jurgen Polle). The *D. salina/D. bardawil*

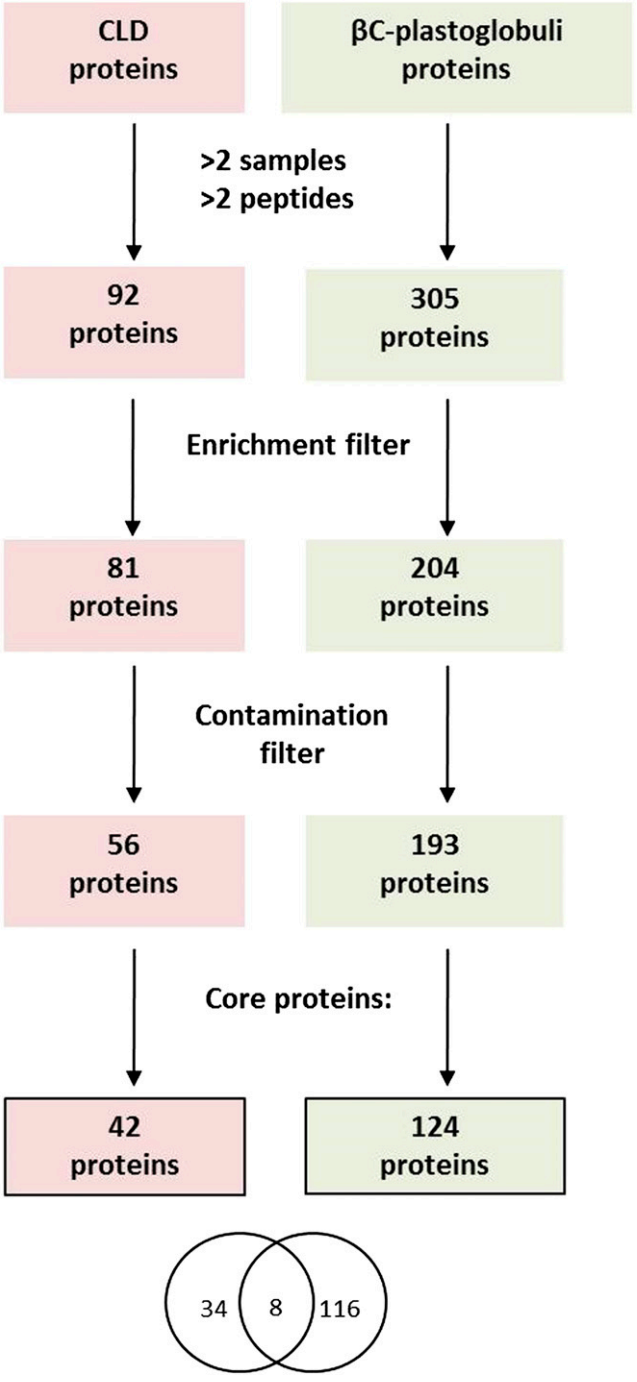

Figure 2. Definition of core proteomes. A total of 305 and 92 unique proteins were identified in βC-plastoglobuli and CLD, respectively. These proteins were passed through two sequential filters: the enrichment filter and the contamination filter. The enrichment filter excluded protein with a lipid droplet to thylakoid ratio less than 2. The contamination filter excluded proteins appearing on the synthetic globule proteome. Totals of 193 and 56 proteins in βC-plastoglobuli and CLD, respectively, passed both filters. Core proteins were defined as having a lipid droplet to thylakoid ratio greater than 10 and more than two peptides or a lipid droplet to thylakoid ratio greater than 4 and more than nine peptides. The final core proteomes comprise 42 and 124 core proteins in CLD and βC-plastoglobuli, respectively.

proteome database comprises 83,694 proteins (more than 50 amino acids) with 20,068 annotated proteins (average length of 318 amino acids). Functional annotation of the proteins was achieved by running all sequences in the Blast2GO program.

A total of 570 proteins were identified in all our lipid droplet samples. Proteins with at least two peptides in at least two biological repeats were analyzed. A total of 305 and 92 unique proteins were identified in βC-plastoglobuli and CLD fractions, respectively, of which 154 and 13 were contained in both the AmBc and SDS extracts (see scheme in Fig. 1).

In order to identify contaminating proteins, we added a novel control based on supplementation of synthetic lipid droplets to control cells during the preparation: control *D. bardawil* cells (nitrogen sufficient) were lysed as described above in the presence of added triolein synthetic lipid droplets. These lipid droplets were isolated by Suc density gradient centrifugation; their proteins were extracted and analyzed as above. This protein preparation served as a contamination filter.

The proteins of βC-plastoglobuli and CLD fractions were compared with triolein synthetic droplet proteins. Common proteins also contained in the latter fraction yielding a similar number of peptides were eliminated as contaminants. The protein abundance of all residual proteins in all lipid droplet fractions was next compared with the protein abundance of the corresponding proteins in the chloroplast membrane proteome (Thylakoids). For βC-plastoglobuli, proteins with enrichment ratios of less than 10 (lipid droplet/Thylakoids < 10) and having less than four identified peptides, or, alternatively, having less than 5-fold enrichment and 10 peptides, were excluded. For CLD proteins, proteins having enrichment values of less than 10 and at least two identified peptides were excluded. These criteria are more stringent than the criteria set previously for defining the core plastoglobule proteome (Lundquist et al., 2012b). This filter removed many chloroplast-derived proteins from the plastoglobule proteome as well as a lot of enzymes such as Fru-bisP aldolase, previously identified as a plastoglobule protein but later removed by the more stringent criteria set for core proteins (Lundquist et al., 2012b). Another indication that the filters are effective is the fact that the number of common proteins in the two proteomes decreased from 38

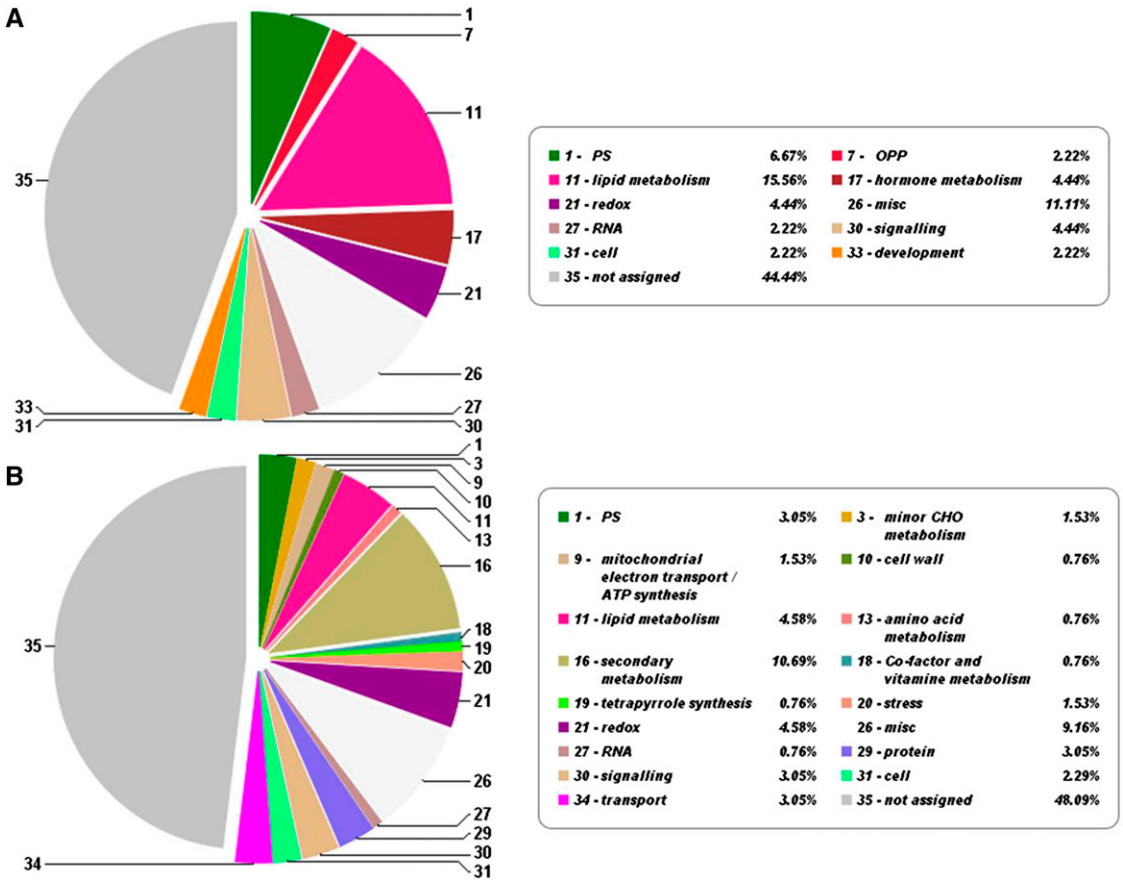

Figure 3. Distribution of protein functional categories. Functional categories are shown for CLD (A) and βC-plastoglobuli (B) core proteomes according to Mercator analysis. CHO, Carbohydrate; misc, miscellaneous; OPP, oxidative pentose phosphate; PS, photosynthesis; redox, oxidation reduction. Numbers represent the protein category according to Mercator, and percentage values represent the number of proteins in this category as a percentage of total proteins.

Table I. *CLD proteome*

Name/Functional Category	Sequence Description	Mass	Sequence Length	No. of Peptides	Fold Change
		kD			
Structural					
AEW43285.1	MLDP	31	282	11	4,866,667
isotig01487.2	SOUL heme-binding protein	43	384	7	8
isotig16296	SOUL heme-binding protein	44	393	22	87
isotig01487.2	SOUL heme-binding protein	43	384	7	8
Membrane remodeling					
CL1Contig7649	Vesicle-inducing protein in plastids (VIPP1)	36	330	8	7
Lipid metabolism					
isotig13730	Diacylglyceryl-trimethylhomo-Ser synthesis protein	79	694	12	1,360,000
F62NEKU02F32Z3	Cyclopropane-fatty acyl-phospholipid synthase	17	154	6	730,000
isotig07478	Acetyl-CoA synthetase-like protein	73	662	14	1,950,000
isotig15711	Acetyl-CoA synthetase-like protein	76	690	6	610,000
isotig06859	Acyl carrier protein (ACP)	16	150	4	41
CL8760Contig1	Glycerophosphodiester phosphodiesterase	42	377	5	570,000
isotig02168.1	Acylglycerol lipase	49	450	2	200,000
Sterol biosynthesis					
isotig07413	Cycloartenol synthase	88	780	20	1,666,667
isotig02727	Squalene epoxidase	58	532	7	520,000
isotig06167.2	Oxysterol-binding family protein	48	426	2	625,000
isotig14763	NAD-dependent steroid dehydrogenase	40	371	2	200,000
Carotenoid metabolism					
isotig08132.2	Retinol dehydrogenase12	41	373	5	690,000
isotig14327	Retinol dehydrogenase14	34	309	9	1,130,000
Quinone metabolism					
CL1Contig605	NADPH:quinone reductase zinc-dependent oxidoreductase	39	364	6	590,000
Glycolysis					
isotig00097.1	Glyceraldehyde-3-phosphate dehydrogenase	42	389	9	29
Amino acid metabolism					
isotig16293	Saccharopine dehydrogenase	47	436	17	98
Catabolism					
CL2520Contig1	α/β-Hydrolase	50	436	3	455,000
isotig03580	Amidase signature enzyme	28	250	21	2,200,000
Oxidation/reduction					
isotig10793	FAD NAD-binding oxidoreductase	26	251	8	1,305,000
isotig16031	Short-chain dehydrogenase	41	371	8	805,000
Ca/endoplasmic reticulum (ER)					
isotig15122	EF hand	20	180	3	240,000
isotig04172.2	Calreticulin precursor	48	429	14	55
Stress related					
CL1Contig4905.1	Hypersensitive-induced response protein	33	299	5	190,000
Nucleic acids					
F60QV6V01CU6OC	RNP-1 like RNA-binding protein	20	165	3	39
isotig01568	Endonuclease exonuclease phosphatase	42	371	6	610,000
Protein modification					
isotig14032.2	Prenyl-Cys methylesterase	53	487	13	1,400,000
Plastid					
F62NEKU02FTJB3	CP12 domain-containing protein1	17	160	4	30
isotig09740	AIG2 family protein	47	433	8	1,055,000
isotig17627	*N*-Acylethanolamine amidohydrolase	66	623	17	442
CX160991.1	Chloroplast precursor	19	180	2	65
CL1Contig7761	Ferredoxin	16	143	2	61
F97XPG002IZM8C	Ferredoxin	13	125	2	29
Unknown					
CL6181Contig1	Hypothetical protein	23	207	4	405,000
isotig16390	Predicted protein	26	247	4	91
CL1Contig3525	Predicted protein	47	438	2	23
isotig16101	Protein (DUF1350)	55	511	4	11
CL1331Contig1	Protein (DUF500)	35	319	6	355,000

Table II. *βC-plastoglobuli proteome*

Name/Functional Category	Sequence Description	Mass	Sequence Length	No. of Peptides	Fold Change
		kD			
Structural					
isotig16296	Carotene globule protein (CGP)	44	206	40	13
CL10820Contig1	SOUL heme-binding protein	29	265	4	48,333
CL17536Contig1	SOUL heme-binding protein	40	353	22	36
isotig01491	SOUL heme-binding protein	37	332	13	71
isotig16144	SOUL heme-binding protein	49	434	24	13
isotig01487.2	SOUL heme-binding protein	43	137	22	13
CL4597Contig1	SOUL3-like protein	29	261	3	55,666
isotig09899	Plastid-lipid-associated protein (PAP)-fibrillin family protein	29	268	10	293,333
isotig15498	PAP-fibrillin family protein	31	279	5	72,000
isotig04183.2	PAP-fibrillin family protein	31	282	7	240,000
isotig15898	Eyespot assembly protein (EYE3), ABC1	118	1,095	21	780,000
isotig17235	Eyespot assembly protein (EYE3), ABC1	129	1,231	35	1,193,330
CL745Contig4	ABC1	35	315	9	286,667
isotig17483	ABC1	96	876	34	1,083,330
CL1Contig10490.1	ABC1	66	634	18	573,333
isotig16860	ABC1	96	887	4	119,500
isotig06232	ABC1	63	567	23	653,333
isotig16432	ABC1	73	653	43	1,483,330
isotig17448	ABC1	91	824	19	436,667
isotig14084	ABC1	81	734	13	333,333
Carotenoid metabolism					
isotig15955	Phytoene desaturase	66	596	29	4
CL4186Contig1	Lycopene cyclase (LCY)	67	605	22	65
isotig16154	LCY	74	692	25	833,333
isotig16249	ζ-Carotene desaturase (ζCDS)	65	587	22	12
CL7381Contig1	ζCDS	43	388	4	80,000
302140351	ζCDS	64	576	3	81,666
CL1Contig352.2	Carotene isomerase	39	367	12	426,667
contig23620	Carotene isomerase	29	269	7	21
isotig11982	Carotene biosynthesis-related protein	24	229	3	58,000
isotig04110	Zeaxanthin epoxidase	47	440	12	326,667
isotig14327	Retinol dehydrogenase14	34	309	6	143,333
isotig06854	Pheophorbide A oxygenase	66	593	6	115,000
Tocopherol biosynthesis					
isotig16794.2	Tocopherol vitamin E cyclase1 (VTE1)	50	601	15	9
CL1Contig3478	γ-Tocopherol methyltransferase	37	349	6	136,667
Lipid metabolism					
isotig07478	Acetyl synthetase	73	267	15	296,666
isotig15851	Phytyl ester synthase (PES)	87	781	26	926,667
isotig04015	Phytyl ester synthase (PES)	100	918	11	450,000
CL1Contig10166.1	Phytyl ester synthase (PES)	102	936	24	580,000
CL4703Contig1	Esterase/lipase/thioesterase family protein	57	509	6	180,000
GBSVTBZ01B1VF9	Glycolipid transfer protein	17	155	4	69,500
isotig16199.1	3-β-Hydroxysteroid dehydrogenase isomerase	31	285	11	12
isotig17627	*N*-Acylethanolamine amidohydrolase	66	519	16	84
Membrane remodeling					
CL1Contig6738	Plant synaptotagmin	51	480	4	29,666
CL1Contig7649	VIPP1	36	330	17	7
Hydrolases/lyases					
isotig08376	α/β-Hydrolase	21	187	5	130,000
CL1Contig4447	Hydrolase-like protein	36	331	15	14
isotig03580	Amidase signature enzyme	28	250	16	546,667
isotig08435	RNase p protein component	22	198	3	72,000
isotig19825	Peptidase M48	41	373	5	123,333
isotig13720	Signal peptide peptidase	81	769	5	105,000
Chlorophyll/cofactors/ vitamins					

(*Table continues on following page.*)

Table II. (*Continued from previous page.*)

Name/Functional Category	Sequence Description	Mass	Sequence Length	No. of Peptides	Fold Change
CL1Contig605	NADPH:quinone reductase zinc-dependent oxidoreductase	39	364	8	176,667
isotig17345.1	Methylenetetrahydrofolate reductase	44	411	4	47
CL2130Contig1	Divinyl protochlorophyllide *a* 8-vinyl reductase	47	431	7	170,000
CL5220Contig1	Ubiquinone menaquinone biosynthesis methyltransferase	44	406	8	263,333
isotig13689	MPBQ/MSBQ methyltransferase2	37	328	13	19
Signaling					
isotig20674	GTP-binding protein	23	207	8	240,000
isotig06897.1	Rab2 family small GTPase	25	221	11	213,333
isotig16758	Rab11 family small GTPase	25	225	7	119,500
CL77Contig4	Extracellular calcium-sensing receptor	43	409	10	4
isotig04273	Rho GTPase-activating protein	49	467	3	97,000
Protein kinases/phosphatases					
isotig14775	Tyr phosphatase family	49	451	9	220,000
Methyltransferases					
isotig04348.2	*S*-Adenosyl-L-Met-dependent methyltransferase	40	372	8	143,333
CL1Contig335	Generic methyltransferase	61	167	26	30
Oxidoreductases					
isotig20240	Glc-methanol-choline oxidoreductase	67	625	18	17
isotig16059.1	Thiol-disulfide oxidoreductase DCC	52	473	5	155,000
isotig14675	Oxidoreductase-like protein	50	470	20	18
CL1Contig4961.1	Amine oxidase	62	563	15	346,667
isotig16623	Amine oxidase	63	582	17	666,667
isotig06585	Plastid terminal oxidase	52	449	4	88,666
isotig14010	Short-chain dehydrogenase	36	330	18	37
isotig13659	Aldo/keto-reductase	41	376	20	13
CL5790Contig1	Rossmann fold NAD-binding protein	28	268	3	33,000
CL1Contig7258	Rossmann fold NAD-binding protein	66	617	21	5
CL4625Contig2	NAD(P)-binding protein	35	339	6	180,000
isotig07081	NADH dehydrogenase	71	642	28	14
isotig16044	NADH dehydrogenase	60	570	13	5
Amino acid metabolism					
isotig16293	Saccharopine dehydrogenase	47	2,681	22	31
isotig14128	Saccharopine dehydrogenase	50	457	10	176,667
isotig17511	Saccharopine dehydrogenase	51	479	20	28
isotig15874	Aryl-alcohol dehydrogenase	42	386	30	26
isotig01812.1	AMP-dependent synthetase and ligase	84	782	11	8
Stress related					
isotig16513	Glutathione *S*-transferase	48	430	13	400,000
isotig14874	Harpin-binding protein1	29	267	5	103,333
CL1Contig8605	DNAJ-like protein	49	445	4	69,500
CL1Contig5346	*N*-Acetylmuramoyl-L-Ala amidase	34	303	10	260,000
isotig16141	Early light-induced protein	20	187	5	120,000
Transport					
isotig15740	ABC transporter	96	876	8	29
isotig16443	Mitochondrial carrier protein	46	429	7	185,000
CL5834Contig2	Nuclear transport factor2	19	173	7	170,000
isotig13261	Arsenical pump-driving ATPase-like	82	758	4	69,500
ER/Ca					
CL3422Contig1	Cytochrome P450	60	552	9	175,000
Cell wall					
isotig18214	UDP-GlcNAc pyrophosphorylase	145	1,362	22	6
Photosynthesis					
HO703428.1	Chlorophyll *a*/*b*-binding protein	30	277	3	92,000
isotig02840	Chlorophyll *a*/*b*-binding protein	32	301	10	6
383930352	Cytochrome F	31	287	14	7
isotig16365	Thioredoxin family protein	42	383	17	14
Unknown					
isotig14695	α/β-Fold family protein	43	394	4	88,666

(*Table continues on following page.*)

Table II. (*Continued from previous page.*)

Name/Functional Category	Sequence Description	Mass	Sequence Length	No. of Peptides	Fold Change
isotig16434	SLR1470 gene product	31	274	11	7
isotig13386	Membrane protein	62	593	11	196,667
isotig08678.2	Predicted protein	27	243	3	57,666
isotig05803	Predicted protein	33	297	5	80,000
isotig16288	Predicted protein	30	273	9	303,333
isotig15794	Predicted protein	31	295	6	180,000
isotig06249	Predicted protein	51	475	5	206,667
isotig08618	Predicted protein	9	82	4	96,333
CL1Contig10414	Predicted protein	15	138	5	11
isotig14932	Predicted protein	27	245	3	58,000
isotig15746.1	Predicted protein	36	325	7	206,667
isotig14316	Hypothetical protein	30	273	10	343,333
isotig11579	Hypothetical protein	25	225	6	190,000
contig00323	Hypothetical protein	35	314	9	200,000
CL4228Contig1	Hypothetical protein	23	211	15	543,333
isotig16545	Hypothetical protein	32	300	13	416,667
contig16530.1	Hypothetical protein	28	259	4	96,333
CL1Contig9415.1	Hypothetical protein	23	214	8	16
isotig15720	Hypothetical protein	35	322	19	27
isotig15617.1	Hypothetical protein	42	376	13	5
isotig21337	Hypothetical protein	12	113	3	88,666
isotig06777	Hypothetical protein	111	1,009	13	4
isotig20329.2	Hypothetical protein	47	415	4	11
CL6726Contig1	Protein (DUF393)	27	244	5	166,333
isotig16101	Protein (DUF1350)	55	511	22	36
isotig13969.1	Protein (DUF1997)	38	344	9	15
isotig14136	Protein (DUF4336)	56	502	11	5

to eight after applying the filtration. The risk of applying such stringent filters is that it may exclude minor potentially important proteins such as protein kinases or proteins involved in signaling. A total of 124 and 42 proteins in the βC-plastoglobuli and CLD fractions passed both filters (see scheme in Fig. 2; all core sequences are available in Supplemental Fig. S1 [CLD] and Supplemental Fig. S2 [βC-plastoglobuli]). Very few chloroplast-derived proteins still escaped the filter, such as ferredoxins and a chloroplast precursor in the CLD list, for unknown reasons. Ignoring these few proteins as well as predicted proteins or proteins with no assigned function resulted in a list of 84 and 28 proteins in the βC-plastoglobuli and CLD proteomes, respectively. The finding that only eight common proteins were identified in both fractions (Fig. 2) suggests that the two proteomes are distinct and have different origins.

Core CLD and βC-Plastoglobuli Proteomes

Functional category diagrams of the two lipid droplet proteomes (Fig. 3) show that they differ in their major functional categories: in CLD, the major category is lipid-metabolizing enzymes, whereas in βC-plastoglobuli, it is secondary metabolism enzymes.

Tables I and II summarize the predicted proteins identified in the CLD and βC-plastoglobuli fractions, respectively. Tables III and IV show comparisons between the proteomes of *D. bardawil* CLD and βC-plastoglobuli and between the proteomes of two *Chlamydomonas reinhardtii* cytoplasmic droplets (Moellering and Benning, 2010; Nguyen et al., 2011), Arabidopsis (*Arabidopsis thaliana*) plastoglobule full and core proteomes (Lundquist et al., 2012b), *C. reinhardtii* eyespot (Schmidt et al., 2006), and bell pepper chromoplasts (Siddique et al., 2006).

As clearly seen from the comparisons, the *D. bardawil* CLD and βC-plastoglobuli proteomes resemble different proteomes: *D. bardawil* CLD mostly resemble cytoplasmic droplets from *C. reinhardtii*, whereas *D. bardawil* βC-plastoglobuli resemble Arabidopsis plastoglobules and *C. reinhardtii* eyespot proteomes.

For example, the βC-plastoglobuli contain PAP-fibrillins, SOUL heme-binding proteins, Activity of bc1 complex (ABC1-kinase) kinase proteins, VTE1, and PESs, which may be considered as protein markers of plastoglobules in plants (Nacir and Bréhélin, 2013). Other proteins that have also been identified in other plastoglobules include acyltransferase, peptidase M48, aldo-keto-reductase, harpin-binding protein, and Rossmann fold NAD(P)-binding domain protein. We also identified in the *D. bardawil* βC-plastoglobuli proteome most β-carotene biosynthesis enzymes, including phytoene desaturase (PDS), lycopene cyclase (LCY), and ζCDS, part of which were identified previously in eyespot and bell pepper chromoplast proteomes, which also accumulate carotenoids (Schmidt et al., 2006; Siddique et al., 2006; Ytterberg

Table III. *Comparison of CLD with C. reinhardtii CLD*
Arabidopsis plastoglobules were added as a reference.

Protein Name	*D. bardawil* CLD	*C. reinhardtii* CLD[a]	*C. reinhardtii* CLD[b]	Arabidopsis Core Plastoglobules[c]
MLDP	AEW43285.1	338,214	192,823	
Diacylglyceryl-trimethylhomo-Ser synthesis protein	isotig13730	77,062	77,062	
Cyclopropane-fatty acyl-phospholipid synthase	F62NEKU02F32Z3	399,825	119,132	
Acetyl synthetase-like protein	isotig07478	380,622		
Acetyl-CoA synthetase-like protein	isotig15711	377,723	123,147	
Cycloartenol synthase	isotig07413	196,409	116,558	
Squalene epoxidase	isotig02727	381,157		
Retinol dehydrogenase14	isotig14327	390,185		
Retinol dehydrogenase12-like	isotig08132.2	176,680	176,680	
NADPH:quinone reductase zinc-dependent oxidoreductase	CL1Contig605			
Saccharopine dehydrogenase	isotig16293			
Glyceraldehyde-3-phosphate dehydrogenase	isotig00097.1	140,618	140,618	
Calreticulin precursor	isotig04172.2		78,954	
Prenyl-Cys methylesterase	isotig14032.2	343,002		
Unknown function	isotig16390			
Protein (DUF1350)	isotig16101		121,991	AT3G43540.1
NAD-dependent steroid dehydrogenase-like	isotig14763	58,501	58,501	
α/β-Hydrolase fold protein	CL2520Contig1	330,619	173,167	
RNP-1-like RNA-binding protein	F60QV6V01CU6OC	184,151	184,151	
Chloroplast precursor	CX160991.1			
Ferredoxin	CL1Contig7761		159,161	
SOUL heme-binding protein	isotig01487.2			

[a]Nguyen et al. (2011). [b]Moellering and Benning (2010). [c]Lundquist et al. (2012b).

et al., 2006). In addition, we identified several unique proteins in the *D. bardawil* βC-plastoglobuli: the major lipid-associated protein CGP (Katz et al., 1995; Davidi et al., 2014), the eyespot assembly protein EYE3 (Boyd et al., 2011), the vesicle-inducing plastid protein VIPP1, and plant synaptotagmin. The proteome includes several enzymes involved in the synthesis and/or degradation of lipids, carotenoids, terpenoids, quinones, enzymes involved in carbohydrate and energy metabolism, stress-related proteins, protein kinases and phosphatases, as well as signaling proteins, suggesting diverse metabolic and regulatory roles (Tables II and IV). A comprehensive Kyoto Encyclopedia of Genes and Genomes metabolic map showing the identified enzymes in the relevant metabolic pathways is depicted in Supplemental Figure S3A.

CLD, in contrast, contain a much smaller and mostly different protein composition: a different major lipid-droplet-associated protein (MLDP), characteristic of green algae (Davidi et al., 2012), and several glycerolipid and sterol biosynthesis enzymes identified earlier in cytoplasmic droplets of *C. reinhardtii*, including diacylglyceryl trimethyl homo-Ser synthesis protein (betaine lipid synthase), a protein marker of CLD in green algae involved in the synthesis of trimethylhomo-Ser diacylglycerol (DGTS), cyclopropane-fatty-acyl-phospholipid synthase, acetyl-CoA synthase, squalene epoxidase, and NAD-dependent steroid dehydrogenase (Tables I and III). Supplemental Figure S3B depicts the identified enzymes in the relevant metabolic pathways.

Sequence Analysis and Comparisons with Other Gene Families

Major Structural Proteins: CGP, MLDP, and Fibrillins

CGP is the major plastoglobule-associated protein in *D. bardawil* (Katz et al., 1995). It differs in sequence from sequenced green algae MLDPs, fibrillins, and plant oleosins, suggesting that it has a different origin. However, we identified several ortholog proteins whose functions are not known in other microalgae and plants (Fig. 4A). As we noted earlier (Davidi et al., 2014), the sequence of CGP reveals partial homology to SOUL heme-binding proteins. The βC-plastoglobuli proteome also contained four PAP-fibrillin sequences, which show clear similarity to plastoglobulins in plants and algae (PAP-FIBRILLIN1 [FBN1], FBN7, and FBN8; Fig. 4B). Two of the four fibrillins most closely resemble homologs in the eyespot proteome of *C. reinhardtii*. In contrast to plant and green algae such as *C. reinhardtii*, in which fibrillins are the major lipid-associated proteins (Ytterberg et al., 2006; Singh and McNellis, 2011; Lundquist et al., 2012b), in the *D. bardawil* proteome they are minor constituents compared with CGP. In earlier work, we found that proteolysis of CGP destabilizes βC-plastoglobuli, suggesting that CGP may have a similar role to fibrillins in stabilizing the plastoglobules (Katz et al., 1995; Youssef et al., 2010; Singh and McNellis 2011). We did not identify in our proteomes homologs of green algal oleosins (Huang et al., 2013), *Chlorella* spp. caleosin (Lin et al., 2012), *Nannochloropsis* spp. hydrophobic lipid droplet surface protein (Vieler

Table IV. *Comparison of βC-plastoglobuli with C. reinhardtii eyespot, Arabidopsis plastoglobules, and bell pepper chromoplasts*

C. reinhardtii CLD were added as reference.

Protein Name	*D. bardawil* βC-Plastoglobuli	*C. reinhardtii* CLD[a]	Eyespot[b]	Arabidopsis Core Plastoglobules[c]	Arabidopsis Full Plastoglobules[c]	Bell Pepper Chromoplast[d]
SOUL domain-containing protein	isotig16144		C_970031	AT3G10130.1	AT3G10130.1	
ABC1	isotig17483			AT3G24190.1	AT3G24190.1	
ABC1	isotig06232			AT5G05200.1	AT5G05200.1	
ABC1	isotig16432		C_230061	AT4G31390.1	AT4G31390.1	
ABC1	isotig17448		C_110160	AT1G79600.1	AT1G79600.1	
EYE3	isotig17235		g6053.t1*			
EYE3	isotig15898		Cre02.g105600.t2*			
PDS	isotig15955		C_490019		AT4G14210.1	AAK64084.1
ζCDS	isotig16249					AAB35386.1
ζCDS	302140351					
Carotene biosynthesis-related protein	isotig11982					
Zeaxanthin epoxidase	isotig04110					
Lycopene β-cyclase	CL4186Contig1					Q42435.1
Retinol dehydrogenase14	isotig14327	145,585			AT1G03630.1	
Tocopherol cyclase	isotig16794.2			AT4G32770.1	AT4G32770.1	
3-β-Hydroxysteroid dehydrogenase isomerase	isotig16199.1		C_100060	AT2G34460.1	AT2G34460.1	
Acetyl synthetase-like protein	isotig07478	123,147	C_7940001			
Acyltransferase-like protein chloroplastic-like	isotig15851			AT1G54570.1	AT1G54570.1	
PAP-fibrillin family protein	isotig04183.2		C_250022	AT2G46910.1	AT2G46910.1	CAA65784.1
PAP-fibrillin family protein	isotig15498		C_580038			
Harpin-binding protein1	isotig14874		C_2460003	AT3G23400.1	AT3G23400.1	AAR26481.1
Rab11 family small GTPase	isotig16758					NP_563750.2
Rab2 family small GTPase	isotig06897.1	148,836				
Protein kinase domain-containing protein	isotig14084			AT3G07700.3	AT3G07700.1	
AMP-dependent synthetase and ligase	isotig01812.1					AAL29212.1
Saccharopine dehydrogenase	isotig17511				AT5G39410.1	
Saccharopine dehydrogenase-like protein	isotig14128		C_970001		AT1G50450.1	
Type II calcium-dependent NADH dehydrogenase	isotig07081	133,334				
Short-chain dehydrogenase	isotig14010		C_2440006			BAB93004.1
NADH dehydrogenase	isotig16044		C_820024	AT5G08740.1	AT5G08740.1	
Rossmann fold NAD-binding domain-containing protein	CL5790Contig1	118,820				
Rossmann fold NAD-binding domain-containing protein	CL1Contig7258				AT4G18810.1	
NAD(P)-binding protein	CL4625Contig2			AT1G32220.1	AT1G32220.1	
NADPH:quinone reductase zinc-dependent oxidoreductase	CL1Contig605				AT4G13010.1	
Peptidase M48	isotig19825		C_240088	AT3G27110.1	AT3G27110.1	
Signal peptide peptidase	isotig13720				AT1G73990.1	
UDP-GlcNAc pyrophosphorylase	isotig18214		C_1400008			
Ubiquinone menaquinone biosynthesis methyltransferase	CL5220Contig1		C_390049			
Generic methyltransferase	CL1Contig335		C_290078			
γ-Tocopherol methyltransferase	CL1Contig3478	119,132	C_220002		AT4G33110.1	
MPBQ/MSBQ methyltransferase2	isotig13689	129,760			AT3G63410.1	
S-Adenosyl-L-Met-dependent methyltransferase	isotig04348.2			AT2G41040.1	AT2G41040.1	
N-Acetylmuramoyl-L-Ala amidase	CL1Contig5346	184,328	C_80056			
Aldo/keto-reductase	isotig13659		C_190016	AT1G06690.1	AT1G06690.1	

(*Table continues on following page.*)

Table IV. (*Continued from previous page.*)

Protein Name	*D. bardawil* βC-Plastoglobuli	*C. reinhardtii* CLD[a]	Eyespot[b]	Arabidopsis Core Plastoglobules[c]	Arabidopsis Full Plastoglobules[c]	Bell Pepper Chromoplast[d]
Thiol-disulfide oxidoreductase DCC	isotig16059.1		C_140123			
Plastid terminal oxidase	isotig06585					
Amine oxidase	CL1Contig4961.1		C_230123			
Pheophorbide *a* oxygenase	isotig06854				AT2G24820.1	AAL32300.1
Glutathione *S*-transferase	isotig16513				AT5G44000.1	NP_199315.1
Divinyl protochlorophyllide *a* 8-vinyl reductase	CL2130Contig1		C_1330031			
Chlorophyll *a*/*b*-binding protein chloroplastic-like	isotig02840	130,414	C_530002		AT4G10340.1	
Cytochrome P450	CL3422Contig1				AT5G07990.1	
Extracellular calcium-sensing receptor	CL77Contig4		C_1010018		AT5G23060.1	
Cytochrome F	383930352		NP_958358		ATCG00540.1	
Chlorophyll *a*/*b* binding	HO703428.1	184,810	C_10030		AT2G40100.1	
DNAJ-like protein	CL1Contig8605		C_490015		AT1G80030.1	
Mitochondrial carrier domain-containing protein	isotig16443	159,938	C_1540001			
GTP-binding protein	isotig20674	81,259	C_10830001			
Thioredoxin family protein	isotig16365				AT5G03880.1	
Protein DUF1350	isotig16101	121,991	C_1670026	AT3G43540.1	AT5G47860.1	
Protein DUF393	CL6726Contig1			AT1G52590.1		
Predicted protein (*C. reinhardtii*)	CL1Contig10414		C_210162			
Hypothetical protein	contig16530.1					
Hypothetical protein	isotig16545		C_370103			
Hypothetical protein	isotig14316					
Hypothetical protein	isotig15617.1		C_10188			
Hypothetical protein	isotig06777		C_190173			
Hypothetical protein	CL1Contig9415.1	148,810	C_1250029			
Hypothetical protein	isotig15720		C_1550001			
Hypothetical protein	isotig21337		C_120189			

[a]Nguyen et al. (2011). [b]Schmidt et al. (2006). [c]Lundquist et al. (2012b). [d]Siddique et al. (2006).

et al., 2012), or the avocado (*Persea americana*) lipid droplet-associated proteins (Horn et al., 2013).

ABC1 Kinases

ABC1 kinases, belonging to the atypical protein kinase superfamily, are ubiquitous proteins in plant and algal plastoglobules (Lundquist et al., 2012a), and until recently their function was not known (Nacir and Bréhélin, 2013). However, recent studies showed that the function of the plastoglobule ABC1 kinase ABCK3 may be the regulation of chloroplast prenylquinone metabolism and also regulation of the activity of the tocopherol cyclase VTE1 (Manara et al., 2013), likely by phosphorylation (Martinis et al., 2013), and that the ABC1 kinase complex ABCK1/3 contributes to plastoglobule function in prenyl-lipid metabolism, stress response, and thylakoid remodeling (Lundquist et al., 2013). We identified nine distinct ABC1 kinase sequences in the *D. bardawil* βC-plastoglobuli proteome. Phylogenetic analysis shows that five of these proteins belong to ABC1 subgroups K1, K3, K5, K6, and K9, identified as plastoglobule proteins in plants and algae (Fig. 5). Two other sequences closely resemble proteins identified as eyespot assembly protein EYE3 in *C. reinhardtii* (ABC1-EYE3; Fig. 5). EYE3 is a Ser/Thr kinase belonging to the ABC1 superfamily. A recent study localized EYE3 in eyespot lipid droplets in *C. reinhardtii* and proposed that this protein is involved in pigment granule biogenesis (Boyd et al., 2011). The identification of two homologs of EYE3 in high abundance (21 and 35 peptides) and high enrichment in βC-plastoglobuli suggests that they are integral core components of βC-plastoglobuli in *D. bardawil* and may be involved in their biogenesis or structural stabilization.

Two additional sequences, which have homologs in *C. reinhardtii*, have not been categorized previously as plastoglobular proteins (ABC1-X).

SOUL Heme-Binding Proteins

SOUL heme-binding proteins were identified in higher plant plastoglobuli (Ytterberg et al., 2006; Lundquist et al., 2012b) and in green algae eyespot (Schmidt et al., 2006; Kreimer, 2009) proteomes, whose function is unknown. In the *D. bardawil* plastoglobule proteome, we identified five distinct SOUL heme-binding protein sequences, which do not resemble CGP but show clear homology to plastoglobule and eyespot proteins in other

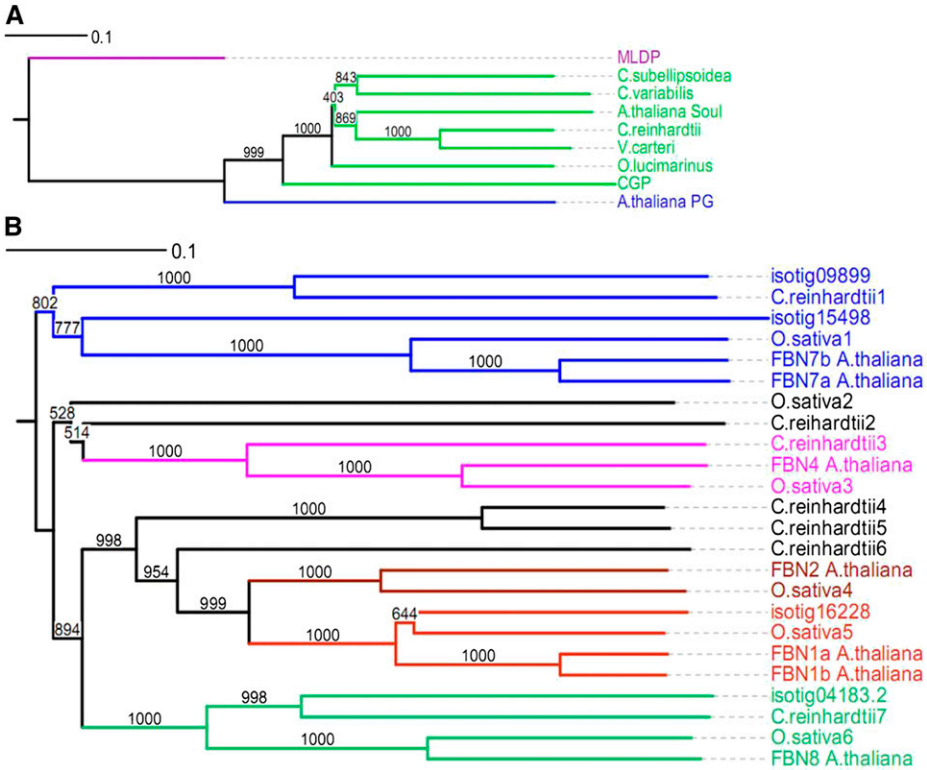

Figure 4. Phylogenetic tree of CGP and PAP-fibrillin in βC-plastoglobuli. A, Phylogenic tree of CGP compared with sequences from other green algae (*Coccomyxa subellipsoidea*, *C. reinhardtii*, *Vovlox carteri*, *Ostreococcus lucimarinus*, and *Chlorella variabilis*) and plants (Arabidopsis). MLDP was added as a reference. Sequence names followed by NCBI accession numbers are as follows: *C.subellipsoidea* (EIE18519.1), *C. reinhardtii* (XP_001691398.1), *V. carteri* (XP_002947474.1), *O. lucimarinus* (XP_001418356.1), *C. variabilis* (EFN56543.1), *A. thaliana*_PG (ABG48434.1), *A. thaliana*_Soul (NP_001190345.1). B, Phylogenetic tree of PAP-fibrillin of βC-plastoglobuli together with proteins from Arabidopsis, rice, and *C. reinhardtii*. Sequence names followed by NCBI accession numbers are as follows: *C.reinhardtii*1 (XP_001698259.1), *C.reinhardtii*2 (XP_001693298.1), *C.reinhardtii*3 (XP_001702245.1), *C. reinhardtii*4 (XP_001698968.1), *C. reinhardtii*5 (XP_001698965.1), *C. reinhardtii*6 (XP_001692028.1), *C. reinhardtii*7 (XP_001690132.1), FBN1a_*A. thaliana* (AT4G04020.1), FBN1b_*A. thaliana* (AT4G22240.1), FBN2_*A. thaliana* (AT2G35490.1), FBN4_*A. thaliana* (AT3G23400.1), FBN7a_*A. thaliana* (AT3G58010.1), FBN7b_*A.thaliana* (AT2G42130.4), FBN8_*A. thaliana* (AT2G46910.1), *O. sativa*1 (NP_001054180.1), *O. sativa*2 (EEE61457.1), *O. sativa*3 (NP_001068210.1), *O. sativa*4 (Q7XBW5.1), *O. sativa*5 (AAO72593.1), *O. sativa*6 (EEE51252.1).

algae (Tables II and IV; Supplemental Fig. S2 in Davidi et al., 2014). Of particular interest is a SOUL3 heme-binding protein, homolog of a SOUL3 recently identified in the eyespot of *C. reinhardtii*, proposed to act in the organization and cellular positioning of the eyespot (Schulze et al., 2013). Interestingly, one SOUL heme-binding protein was identified also in the CLD proteome.

Acyltransferases and Lipases

Different lipid-metabolizing enzymes were identified in CLD and in the βC-plastoglobuli proteome. Of particular interest for us are enzymes that can contribute to TAG biosynthesis, which was the focus of our recent study (Davidi et al., 2014). We have shown that the synthesis of CLD precedes that of βC-plastoglobuli and that they are made primarily by the de novo synthesis of TAG at the ER, whereas βC-plastoglobuli are made in part from the degradation of chloroplast membrane lipids and in part from the transfer of TAG or of fatty acids from CLD (Davidi et al., 2014). The identification of different lipid-metabolizing enzymes in these lipid droplets can shed light on these processes.

We did not identify any homologs of diacylglycerol acyltransferase (DGAT) or of phospholipid diacylglycerol acyltransferase (PDAT), which are the terminal enzymes in TAG biosynthesis in plants and algae, in the *Dunaliella* spp. lipid droplet proteomes. In this respect, *D. bardawil* seems to differ from *C. reinhardtii*, which was reported to contain PDAT, glycerol-3-phosphate acyltransferase, and lysophospatidic acid acyltransferase (Nguyen et al., 2011). However, in the βC-plastoglobuli proteome, we identified three proteins with close homology to PES from Arabidopsis (Lippold et al., 2012) that belong to the esterase/lipase/thioestesase family (Fig. 6A). These enzymes are induced under stress conditions such as nitrogen deprivation and have a dual function in the degradation of polar lipids and their conversion to TAG.

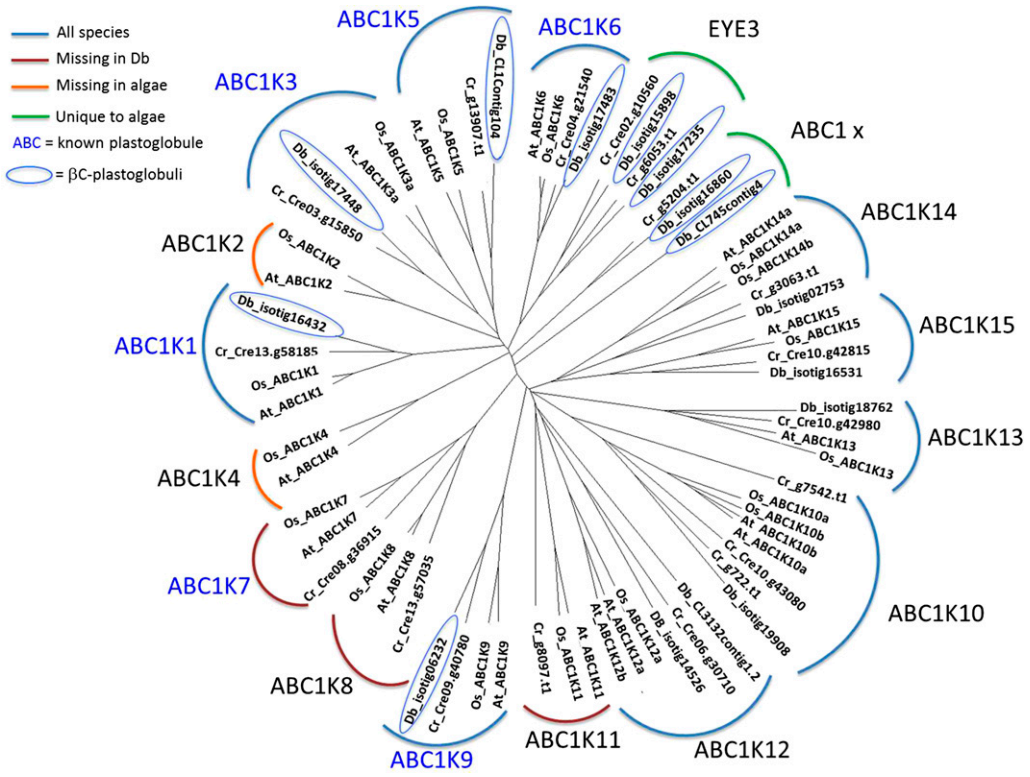

Figure 5. Phylogenetic tree of ABC1 proteins from βC-plastoglobuli. Nine proteins with ABC1 kinase annotation were located in the βC-plastoglobuli. Members of each ABC1 protein family (K1–K15) from rice (Os), Arabidopsis (At), and *C. reinhardtii* (Cr) were used to find orthologs. The sequences were then aligned with both ClustalW (version 2.1) and Muscle (version 3.8.31), and the best alignment was chosen for phylogenetic analysis. Phylogenetic analysis was performed with neighbor joining in ClustalW and ProML (Maximum Likelihood) in Phylip (version 3.69; as described in "Materials and Methods"). Db, *D. bardawil*.

According to our analysis, proteins identified previously in the Arabidopsis plastoglobule proteome as DGAT3 and DGAT4 (Lundquist et al., 2012b) have closer sequence homology to PES than to DGAT. PES homologs were identified also in the lipid droplet proteome from *C. reinhardtii* (Moellering and Benning, 2010; Nguyen et al., 2011), but it is not clear if they originate from cytoplasmatic or plastidic lipid droplets. In view of the finding of PES homologs in the βC-plastoglobuli proteome, but not in the CLD proteome, it is tempting to speculate that these putative PES enzymes are involved in the synthesis of TAG in the chloroplast from the degradation of chloroplast membrane lipids, which creates the βC-plastoglobuli.

The βC-plastoglobuli proteome also contains an acyltransferase, an acyl carrier protein, and a glycolipid transfer protein involved in the exchange of glycolipids between inner and outer membrane leaflets (Mattjus, 2009). The localization of these enzymes in lipid-metabolizing pathways is depicted in Supplemental Figure S3A.

The CLD proteome contains different enzymes involved in the early stages of lipid biosynthesis, such as acetyl-CoA synthase, acyl carrier protein, cyclopropane fatty acyl phospholipid synthase, which modifies acyl chains of phospholipids by the methylation of unsaturated double bonds, and BTA1, involved in the synthesis of trimethylhomo-Ser diacylglycerol. All these enzymes were also identified in a *C. reinhardtii* lipid droplet proteome (Moellering and Benning, 2010; Nguyen et al., 2011; Table III). Two enzymes involved primarily in lipid degradation, glycerophosphodiester phosphodiesterase and acylglycerol lipase, were also identified. These results suggest that CLD are involved in a broad range of lipid biosynthesis and degradation reactions, whereas βC-plastoglobuli are more specifically involved in the degradation of chloroplast membrane lipids and their conversion to TAG during nitrogen deprivation.

Several enzymes identified in CLD may be involved in the degradation of microsomal membrane lipids and of TAG and in the mobilization of fatty acids from CLD into βC-plastoglobuli: glycerophosphodiester phosphodiesterase is a broad-specificity hydrolase that can hydrolyze phosphate ester bonds in phosphatidylcholine, phosphatidylethanolamine, or phosphatidylglycerol to phosphatidic acid, which can be converted into TAG. Acylglycerol lipase and the acyl carrier protein may be involved in the hydrolysis and exchange of fatty acids derived from polar phospholipids or TAG and their transfer from CLD into βC-plastoglobuli. Acetyl-CoA synthase proteins are involved in the early stages of de novo fatty acid biosynthesis (see the localization of these enzymes in lipid-metabolizing pathways in

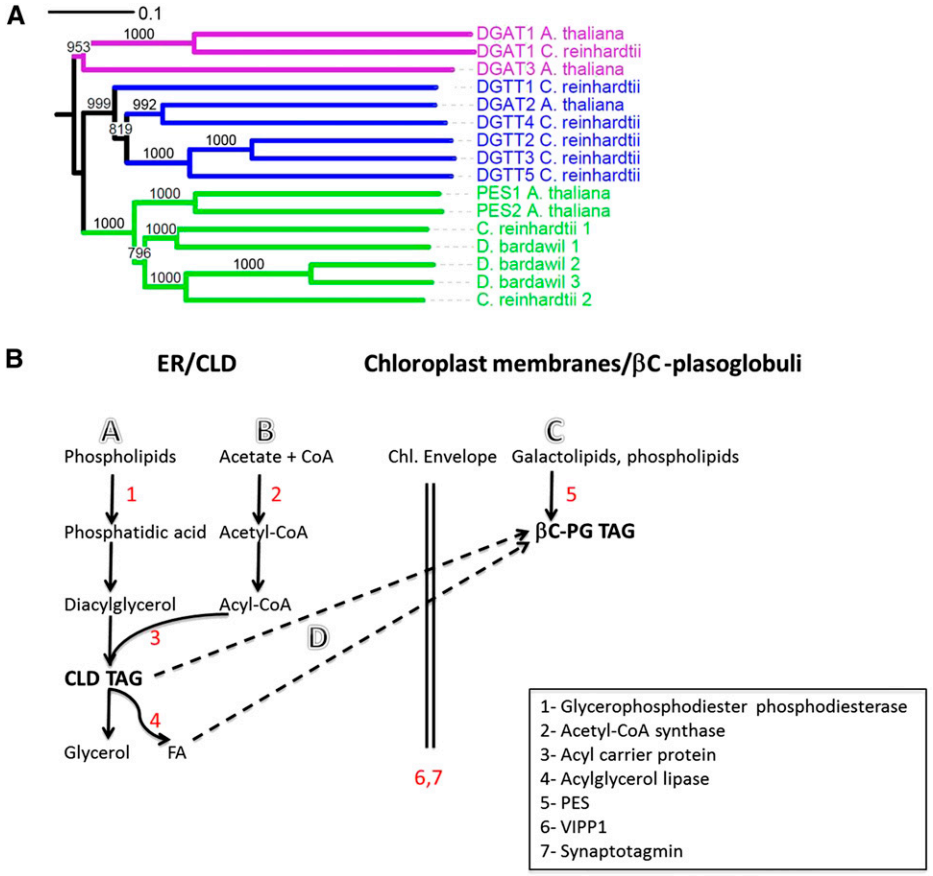

Figure 6. Phylogenetic tree of PES and DGAT in βC-plastoglobuli and schemes of proposed TAG biosynthesis in CLD and βC-plastoglobuli. A, Phylogenic tree of PES and DGAT showing that the three isotigs in *D. bardawil* βC-plastoglobuli show higher homology to PES than to DGAT. *D. bardawil* 1 to 3 refer to isotigs isotig15851, CL1Contig10166.1, and isotig04015, respectively. Sequence names followed by organism and NCBI accession numbers are as follows: PES1_AT1G54570 (Arabidopsis; NP_564662.1), PES2_AT3G26840 (Arabidopsis; NP_566801.1), DGAT1 (Arabidopsis; NP_179535.1), DGAT2_AT3G51520 (Arabidopsis; NP_566952.1), DGAT1_Chlamy (*C. reinhardtii*; from Boyle et al. [2012]), DGTT1_Chlamy (*C. reinhardtii*; AFB73929.1), DGTT2_Chlamy (*C. reinhardtii*; XM_001694852), DGTT4_Chlamy (*C. reinhardtii*; XM_001693137), DGTT5_Chlamy (*C. reinhardtii*; XM_001701615), Chlamy_Cre08.g365950 (*C. reinhardtii*; XP_001696047.1), Chlamy_Cre12.g521650 (*C. reinhardtii*; XP_001696915.1). B, Proposed TAG biosynthesis and mobilization in CLD and βC-plastoglobules in *D. bardawil*. Paths are as follows: A, fatty acid (FA) recycling from phospholipids; B, de novo synthesis; C, fatty acid recycling from galactolipids; and D, CLD TAG recycling.

Supplemental Fig. S3B). Based on the identification of these enzyme homologs and on our recent studies of TAG biosynthesis in these lipid bodies (Davidi et al., 2014), we propose that TAG biosynthesis in CLD is made in part from the recycling of fatty acids from membrane phospholipids and in part from the de novo synthesis of fatty acids, whereas βC-plastoglobuli TAG are produced in part by recycling fatty acids released from chloroplast membrane lipids and in part from fatty acids derived from CLD TAG. A hypothetical scheme summarizing these pathways is shown in Figure 6B.

Sterol Biosynthesis

Three enzymes in sterol biosynthesis were identified in CLD: squalene epoxidase and cycloartenol synthase, central enzymes in the early stages of sterol biosynthesis, and NAD-dependent steroid dehydrogenase, involved in cholesterol biosynthesis. Homologs of these enzymes were identified previously also in lipid droplets from *C. reinhardtii* (Moellering and Benning, 2010; Nguyen et al., 2011; Table III). These results suggest that at least part of the sterol biosynthesis in *Dunaliella* spp. takes place in the CLD. The localization of sterol biosynthesis in plants is not entirely clear: a recent study that tried to localize sterol biosynthesis in Arabidopsis suggests that it is localized in at least three cellular domains: in the ER, at the plasma membrane, and in lipid droplets, which may be homologous to *Dunaliella* spp. CLD (Silvestro et al., 2013).

VIPP1

One of the proteins that were identified in both CLD and in βC-plastoglobuli is VIPP1, which has not been

identified previously in lipid droplets. VIPP1 is a chloroplast membrane-associated protein that is involved in chloroplast envelope and thylakoid membrane biogenesis and stabilization (Vothknecht et al., 2012; Zhang and Sakamoto, 2013). VIPP1 probably evolved from the bacterial phage-shock protein PspA (Westphal et al., 2001), is essential for thylakoid membrane formation (Kroll et al., 2001), and is involved in the transport of proteins across chloroplast thylakoid membranes (Lo and Theg, 2012). Recent studies have shown that VIPP1 and its bacterial homolog PspA associate tightly with membrane lipids and identified the domains in the proteins responsible for their oligomerization and association with chloroplast membranes (Otters et al., 2013). The two *D. bardawil* VIPP1 homologs clearly resemble proteins in other green algae from the Volvocales order (Fig. 7A). In order to verify the existence of VIPP1 in lipid droplets in *D. bardawil*, we analyzed by western analysis the presence of proteins cross-reacting with anti-VIPP1 antibodies. As shown in Figure 7B, protein bands cross-reacting with anti-VIPP1 were indeed identified in protein extracts from both purified CLD and βC-plastoglobuli. Interestingly, two different proteins were identified: whereas CLD contain only one protein of about 30 kD, βC-plastoglobuli seem to contain a major larger protein of about 32 kD. Both proteins seem to be derived from gene CL1Contig7649 by our proteome analysis. These results may suggest that VIPP1 has alternative splicing sites leading to two proteins: a 30-kD protein dominant in CLD and a 32-kD protein dominant in the βC-plastoglobuli.

Proteins Potentially Involved in βC-Plastoglobuli Formation and Stabilization

In a previous study, we showed that the formation of βC-plastoglobuli was preceded by close associations between CLD and chloroplast envelope membranes and by discontinuous envelope membrane staining, which could indicate structural reorganization. If cytoplasmic droplet-derived lipids indeed contribute to the formation of βC-plastoglobuli, it would involve a massive transfer of lipids from CLD to βC-plastoglobuli through the chloroplast envelope membranes. Such a process would possibly involve structural reorganizations in chloroplast envelope membranes. In this study, we identified four potential candidate proteins that might be involved in such an intriguing process: VIPP1, synaptotagmin, SOUL3, and EYE3. Synaptotagmin is a calcium sensor that mediates neurotransmitter release in mammalian synapses by the fusion of neurotransmitter-storing vesicles with the outer cell membranes (Chapman, 2008) and the endosome recycling and trafficking of plant virus genomes in plants (Lewis and Lazarowitz, 2010). The identification of a homolog of this protein in *D. bardawil* βC-plastoglobuli may indicate that it is involved in their biogenesis and/or interactions with chloroplast membranes.

The identification of VIPP1 in both CLD and βC-plastoglobuli may also provide a clue to clarify how they interact with chloroplast envelope membranes leading to transmembrane lipid transfer.

SOUL3 and EYE3, as mentioned above, were localized in eyespot lipid droplets and proposed to be

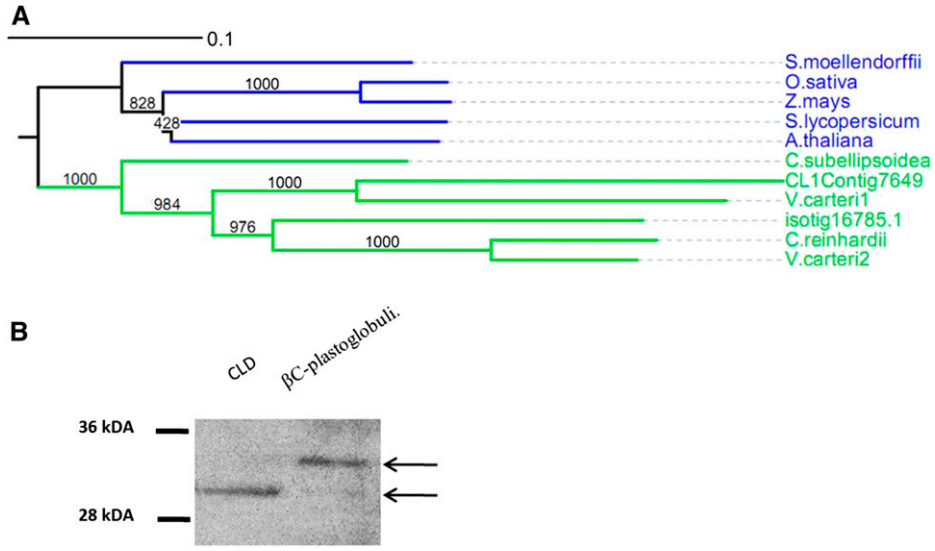

Figure 7. Expression and phylogenetic tree of VIPP1 in CLD and βC-plastoglobuli. A, Phylogenetic tree of VIPP1 from *D. bardawil* CLD and βC-plastoglobuli together with orthologs from plant and green algal VIPP1. Sequence names followed by NCBI accession numbers are as follows: *C. reinhardtii* (XP_001693830.1), *O. sativa* (NP_001045073.1), *A. thaliana* (NP_564846.1), *Z. mays* (*Zea mays*; ACG32836.1), *S. moellendorffii* (*Selaginella moellendorffii*; XP_002970544.1), *S. lycopersicum* (*Solanum lycopersicum*; XP_004250100.1), *V. carteri*1 (XP_002949072.1), *V. carteri*2 (XP_002948865.1), *C. subellipsoidea* (XP_005643904.1). B, Western-blot analysis of protein from CLD and βC-plastoglobuli with VIPP1 antibodies (dilution, 1:1,000) showing one band in CLD and two bands in βC-plastoglobuli.

involved in the biogenesis, stabilization, and targeting of these lipid droplets in *C. reinhardtii*. They may have a similar function in βC-plastoglobuli in *D. bardawil*.

β-Carotene Biosynthesis Enzymes

We identified in the *D. bardawil* proteome one phytoene synthase (PSY) gene, two PDS genes, two LCY genes, four ζCDS genes, and three carotene isomerase genes. In order to clarify the possible involvement of these gene products in β-carotene biosynthesis, we also tested the changes in mRNA expression levels of these genes during nitrogen deprivation in high-light conditions, which induce β-carotene accumulation (Fig. 8A). Interestingly, we found different subcellular localizations and mRNA expression patterns for PSY and for the two PDS genes: PSY was not identified in βC-plastoglobuli and seemed to be restricted to chloroplast membranes; PDS1 was enriched 4-fold in βC-plastoglobuli, whereas PDS2, like PSY, seems to be excluded from βC-plastoglobuli (Fig. 8B). The expression of PSY was greatly increased 6 to 48 h following stress induction, whereas PDS1 appears to be highly expressed continuously, and so is PDS2, but at a lower level. These results suggest that the synthesis of phytoene takes place in chloroplast membranes and that it is activated under stress induction. In contrast, phytoene desaturation takes place in parallel in plastoglobules and in chloroplast membranes by different enzymes. LCY1 and LCY2 both seem to be localized exclusively in plastoglobules (65- and 95,000-fold enrichment, respectively), and appear to be differentially induced after 12 to 24 h (LCY2) or after 96 h (LCY1). The four ζCDS genes reveal the most diverse pattern of expression: ζCDS1 and ζCDS2, localized in βC-plastoglobuli, seem to be differentially expressed 96 to 168 h (ζCDS1) or 12 to 96 h (ζCDS2) after induction, whereas ζCDS3, localized in the βC-plastoglobuli, and ζCDS4, localized in chloroplast membranes, seem to be suppressed during induction.

This complex pattern of localization and expression suggests that part of the β-carotene biosynthesis enzymes is located in chloroplast membranes, whereas others are contained in βC-plastoglobuli, suggesting two parallel biosynthetic pathways.

The finding of only one PSY gene in chloroplast membranes and not in βC-plastoglobuli, and all subsequent

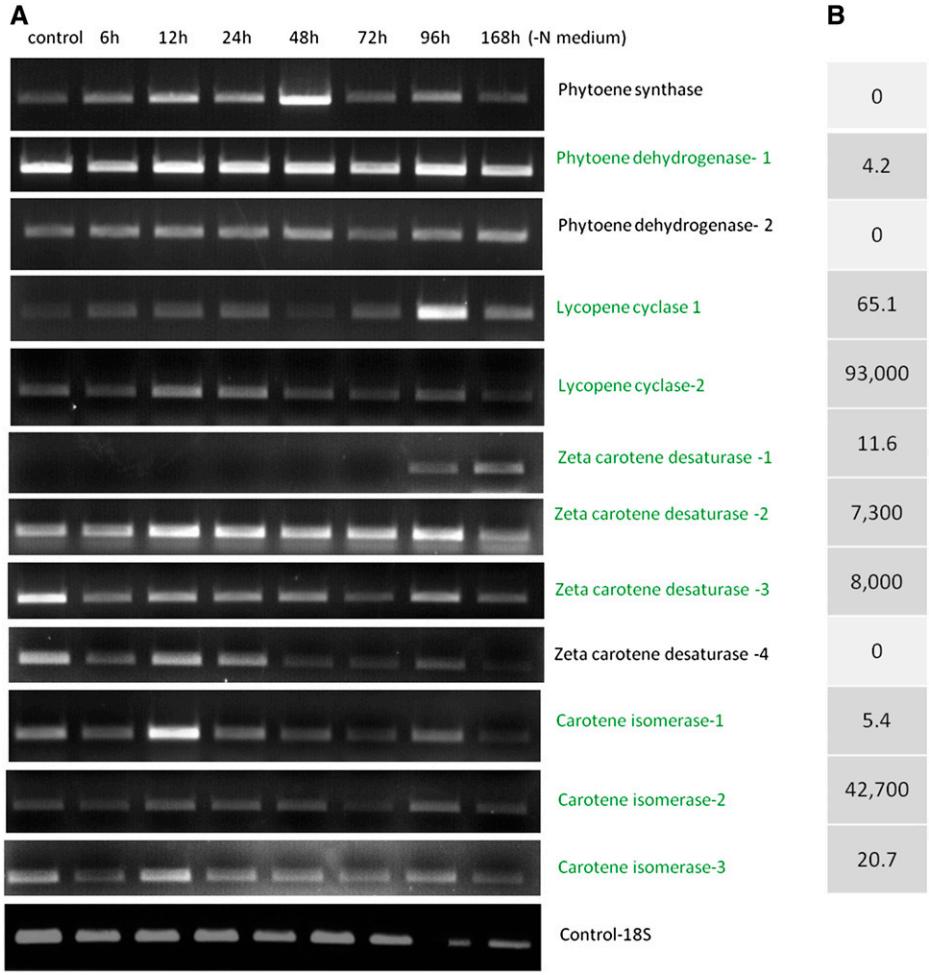

Figure 8. mRNA expression and protein enrichment levels of β-carotene biosynthetic enzymes. A, mRNA expression of β-carotene biosynthetic enzymes in *D. bardawil* nitrogen-deprived (−N) cells. Enzyme names in black are located in chloroplast membranes; enzyme names in green are located in βC-plastoglobuli. Expression of 18S was added as a control. B, Protein enrichment levels. Numbers indicate the protein fold change increase in βC-plastoglobuli compared with chloroplast membranes (fold change calculations are described in "Materials and Methods").

enzymes in the βC-plastoglobuli, suggests that the initial stages of β-carotene biosynthesis in *D. bardawil*, up to phytoene, takes place in chloroplast membranes, whereas all subsequent parts of the biosynthetic pathway occur in the βC-plastoglobuli. This finding is consistent with the fact that phytoene is the first intermediate in the pathway that is lipophilic and would preferentially dissolve in lipid droplets as compared with membranes. Therefore, its transfer from chloroplast membranes to βC-plastoglobuli should be kinetically favored. The finding that phytoene is the only biosynthetic intermediate that accumulates in βC-plastoglobuli at early stages of induction (figure 2A in Davidi et al., 2014) is also in agreement with this hypothesis. The finding of several isoforms of phytoene dehydrogenase (PDH) and ζCDS, one localized in chloroplast membranes and the other in the βC-plastoglobuli, is consistent with the idea of two pathways for β-carotene biosynthesis: a constitutive pathway in chloroplast membranes, for the biosynthesis of β-carotene and light-harvesting accessory xanthophylls, and the inductive pathway in βC-plastoglobuli, for the stress-induced massive accumulation of β-carotene. We also identified several putative carotene isomerases, which may promote the isomerization of all-trans- to 9-cis-β-carotene or of one of its precursors. A model summarizing this proposed biosynthesis pathway is depicted in Figure 9.

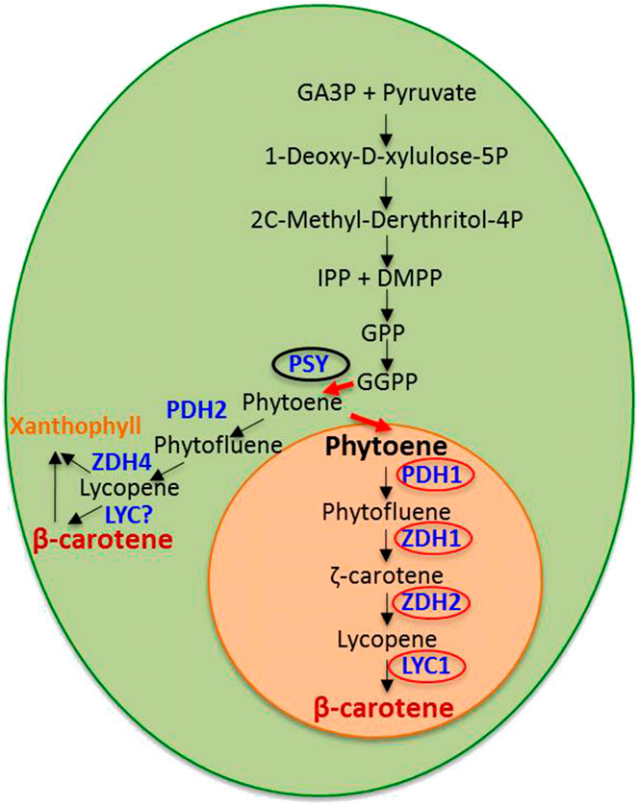

Figure 9. Proposed scheme of β-carotene biosynthesis in *D. bardawil*. Two pathways for β-carotene biosynthesis in *D. bardawil* are a constitutive pathway in the chloroplast (green) and an inducible pathway in the βC-plastoglobuli (orange). DMPP, Dimethylallyl diphosphate; GA3P, glyceraldehyde 3-phosphate; GGPP, geranylgeranyl diphosphate; GPP, geranyl pyrophosphate; IPP, isopentenyl diphosphate; ZDH, ζ-carotene dehydrogenase.

Origin of βC-Plastoglobuli

The question of how βC-plastoglobuli evolved in *D. bardawil* is still a mystery, but the comparison of the βC-plastoglobuli proteome with previously published proteomes of other lipid droplets in microalgae and plants may provide a clue to this interesting question. Logical possible origins are the two types of lipid droplets in green algae chloroplasts: plastoglobules and eyespot lipid droplets. According to their pigment contents, βC-plastoglobuli resemble eyespot lipid droplets, since both contain a similar mixture of 9-cis- and all-trans-isomers of β-carotene. Also, comparison of the proteomes of βC-plastoglobuli with other lipid droplet proteomes shows the highest resemblance to the eyespot (Table IV): notably, βC-plastoglobuli, like the eyespot, contains EYE3 as major proteins, SOUL3 heme-binding protein, similar PAP-fibrillins, β-carotene biosynthesis enzymes, and many other proteins without identified functions, culminating in about 40 homologous proteins. However, βC-plastoglobuli also closely resemble the Arabidopsis plastoglobule in their proteomes. A possible reason why the number of core proteins in these lipid droplets is significantly higher than in plant plastoglobules or in *C. reinhardtii* eyespot globules may be that they combine the functions of both, such as lipid metabolism and β-carotene biosynthesis, respectively.

Did βC-plastoglobuli evolve from the amplification of the eyespot? In this respect, it is noteworthy that, in contrast to all other *Dunaliella* spp. that we studied (including *Dunaliella tertilecta*, *Dunaliella parva*, and *Dunaliella acidophila*), all of which have clearly defined eyespots, visible in light and electron micrographs, we never detected a clear eyespot structure in *D. bardawil*. Based on the above considerations, we propose that *D. bardawil* βC-plastoglobuli have evolved from the disintegration and amplification of the eyespot.

In summary, our work shows that CLD and βC-plastoglobuli in *D. bardawil* have different proteomes, suggesting that they have different functions. Of special note are the different lipid-metabolizing enzymes, which are consistent with different TAG biosynthesis mechanisms reported in our earlier work (Davidi et al., 2014), the identification of distinct β-carotene biosynthesis enzymes in βC-plastoglobuli and in chloroplast membranes, suggesting branching of the inductive metabolic pathway for β-carotene biosynthesis in the βC-plastoglobuli from phytone, and the identification of VIPP1, synaptotagmin, and EYE3, possibly involved in βC-plastoglobuli biogenesis. This work also provides indications that βC-plastoglobuli in *D. bardawil* evolved from eyespot lipid droplets.

MATERIALS AND METHODS

Strain and Growth Conditions

Dunaliella bardawil is an isolated species (Ben-Amotz et al., 1989) deposited at the American Type Culture Collection (no. 30861). Culturing conditions, growth media, and nitrogen limitation induction were as described previously (Davidi et al., 2014).

Preparation of Lipid Droplets and Thylakoid Membranes

Isolation of CLD and βC-plastoglobuli lipid droplets was performed essentially as described previously (Davidi et al., 2014). Thylakoid membranes were isolated as described previously (Finel et al., 1984), and synthetic lipid droplets were obtained as described previously (Davidi et al., 2012). Three biological repeats were prepared from each sample.

Immunoblotting

Proteins from isolated lipid droplets were precipitated in 80% (v/v) acetone (Davidi et al., 2012). Then, the proteins were analyzed by 12% (w/v) SDS-PAGE, blotted to nitrocellulose, immunoblotted with anti-VIPP1 antibodies (a gift from Michael Schroda, Molekulare Biotechnologie und Systembiologie Technische Universität) in a 1:1,000 dilution, and visualized by the horseradish peroxidase-based enhanced chemiluminescence system (homemade, using γ-caproic acid and luminol from Sigma-Aldrich).

cDNA Preparation

Cells precultured for 48 h in complete growth medium were collected by centrifugation, washed once, and cultured in nitrogen-deficient medium. After 0, 6, 12, 24, 32, 48, 72, 96, and 168 h, samples of 10 mL containing 1 to 2×10^7 cells were taken for RNA isolation. The cells were collected by centrifugation, immediately flash frozen in liquid nitrogen, and stored at −80°C for further use. Total RNA was isolated using the Tri Reagent procedure according to the manufacturer's protocol (Molecular Research Center). Independent RNA isolations were conducted for each growth period. Template cDNA was synthesized using 0.1 μg of total RNA in a total volume of 20 μL using the SuperScript kit (Invitrogen). Gene expression of β-carotene enzymes in nitrogen-deprived cells was examined using the following primers: for PSY, 5′-GCGATGCATACAAACC-3′ and 5′-TGTCATCAGTCCCACAGTGC-3′; for PDH (1), 5′-GGCTTGCACATCTTCTTTG-3′ and 5′-TCAGCACAATTTGCTTGAGG-3′; for PDH (2), 5′-TTGATTTCCTTGACCTTCGG-3′ and 5′-ATGATGGACTCACAGCCCTC-3′; for ζCDS (1), 5′-TAAAGAAGGCTTTCAGGCCA-3′ and 5′-GACCACCCAGGATCTTAGCA-3′; for ζCDS (2), 5′-CTTGCTGGTCAAGGATCACA-3′ and 5′-GTGAGCTGAGGGGTGGTAAA-3′; for ζCDS (3), 5′-CATTGGAGGGTGACTCTGGT-3′ and 5′-ACGTCATCGGCGTTTTATTC-3′; for ζCDS (4), 5′-AGCCAAACATCTCAGCGAGT-3′ and 5′-AAGGGTATCATTGTGAGCCG-3′; for LCY (1), 5′-TTCGAACGAAGCATCAAGTG-3′ and 5′-GACAAGAAGTTCGCACACGA-3′; for LCY (2), 5′-GACTCCAGGCAGCAAACTTC-3′ and 5′-AACTCATGGGCAATGACCTC-3′; for carotene isomerase (1), 5′-GTTAGCAGAAGGCTTGACGG-3′ and 5′-CCTCAAACACACTCGCTTCA-3′; for carotene isomerase (2), 5′-GTACGACCTATGGAAGGGCA-3′ and 5′-TGATCAACCCTCTCCGAATC-3′; and for carotene isomerase (3), 5′-CACCTGAGGCACTAACAGCA-3′ and 5′-ACCGGTCGTATTGTTTAGCG-3′. All transcripts were compared with the expression of the 18S control gene.

Protein Extraction for Proteomic Analysis

Proteins were extracted from isolated CLD, βC-plastoglobuli, synthetic lipid droplet, and thylakoid membrane precipitation in 80% acetone overnight at 4°C. Precipitated proteins were pelleted by centrifugation and suspended first in 50 mM AmBc (collected as AmBc samples), then the undissolved protein were suspended in 1% SDS (collected as SDS samples). Proteins were quantified using a bicinchoninic acid kit (Pierce). All samples were subjected to in-solution tryptic digestion. Proteins were first reduced using dithiothreitol (Sigma-Aldrich) to a final concentration of 5 mM and incubated for 30 min at 60°C followed by alkylation with 10 mM iodoacetemide (Sigma-Aldrich) in the dark for 30 min at 21°C. Proteins were then digested using trypsin (Promega) at a ratio of 1:50 (trypsin:protein, w/w) for 16 h at 37°C. Digestions were stopped by the addition of formic acid to a concentration of 1%. The samples were lyophilized and stored at −80°C until further analysis.

Liquid Chromatography

Liquid chromatography/mass spectrometry-grade solvents were used for all chromatographic steps. Each sample was dissolved in 97:3 water:acetonitrile and loaded using splitless nano-ultraperformance liquid chromatography (10,000-p.s.i. nanoAcquity device; Waters) in high-pH/low-pH reverse-phase two-dimensional liquid chromatography mode. Samples were loaded onto a C18 Xbridge column (0.3 × 50 mm, 5-μm particles; Waters). Buffers used were 20 mM ammonium formate, pH 10 (A), and acetonitrile (B). For the cytoplasmic samples, peptides were fractionated using a three-fraction regime. For the pure and chloroplast globules, a seven-fraction method was used. The seven-fraction method included a step gradient of 10.8% B, 13.8% B, 15.8% B, 17.8% B, 20.1% B, 23.4% B, and 65% B. The three-fraction approach induced steps of 13.1% B, 17.7% B, and 65% B. Buffers used in the low-pH reverse phase were water + 0.1% formic acid (A) and acetonitrile + 0.1% formic acid (B). Desalting of samples was performed online using a reverse-phase C18 trapping column (180 μm i.d., 20 mm length, 5 μm particle size; Waters). Peptides were separated using a C18 T3 HSS nano-column (75 μm i.d., 200 mm length, 1.8 μm particle size; Waters) at 0.4 μL min^{-1} and eluted from the column using the following gradient (all v/v): 5% to 30% B in 50 min, 30% to 95% B in 5 min, maintained at 95% for 7 min, and then back to the initial conditions.

Mass Spectrometry

The nanoliquid chromatograph was coupled online through a nanoESI emitter (7 cm length, 10-mm tip; New Objective) to a quadrupole ion mobility time-of-flight mass spectrometer (Synapt G2 HDMS; Waters) tuned to at least 20,000 mass resolution (full width at one-half height) for both MS1 and MS2. Data were acquired using Masslynx version 4.1 in $HDMS^E$ positive ion mode. Ions were separated in the T-Wave ion mobility chamber and transferred into the collision cell, as described (Tenzer et al., 2013). Wave velocity and height were set to 300 m s^{-1} and 0.2 V, respectively. Collision energy was alternated from low to high throughout the acquisition time. In low-energy (MS1) scans, the collision energy was set to 5 eV; it was ramped from 27 to 50 eV for high-energy scans. Mass range was set to 50 to 2,000 Thomsons, with a scan rate set to 1 Hz. A reference compound (Glu-Fibrinopeptide B; Sigma) was infused continuously for external calibration using a LockSpray and scanned every 30 s.

Data Processing, Searching, and Analysis

Raw data processing and database searching were performed using Proteinlynx Global Server (IdentityE) version 2.5.2. Database searching was carried out using the Ion Accounting algorithm described by Li and Godzik (2006).

Data were searched against the *Dunaliella salina/D. bardawil* proteome Weizmann Institute of Science (WIS) combined target and reversed (decoy) database and the list of common laboratory contaminants (www.crapome.org). Trypsin was set as the protease, and one missed cleavage was allowed. Fixed modification was set to carbamidomethylation of Cys, and variable modification was set to oxidation of Met.

All identifications were imported to Scaffold version 3.6. A minimum of two peptides per protein and a protein false discovery rate of 1% were set as minimum identification criteria.

Using Scaffold, the normalized spectral counts were calculated for each protein. Student's *t* test was used for statistical evaluation. Fold changes were calculated based on the normalized spectral counts. The average normalized spectral count of each sample was calculated and divided by the average normalized spectral count of the thylakoid membrane samples. The result was designated as fold enrichment.

Data Set Construction

D. salina ESTs were downloaded from GenBank, limiting the search by the taxid: 3046. A total of 6,811 sequences were found and cleaned using Seqclean (http://sourceforge.net/projects/seqclean/) and then trimmed with Sequencher (version 4.10; Gene Codes). The mRNA sequences from GenBank (106 sequences) and the JGI reads (the good_ESTs files from the following libraries: CGFP, CGFS, CGFY, CBZO, CBZP, CBZS, and CBZT) were added to the cleaned ESTs, and redundancy was reduced with CD-HIT-EST (version 4.5.4). The

sequences were then assembled using TGICL version 2.1 (http://compbio.dfci.harvard.edu/tgi/software/). The resulting sequences, both the assembled contigs (38,156) and the nonassembled singletons (54,122), were translated in six frames, and the longest open reading frame (from stop to stop) was taken. CD-HIT was run on the proteins with a cutoff of 90%, and protein sequences 50 amino acids or longer were taken in a data set called wis90 (76,843 sequences). The JGI assembled reads (454Isotigs.gte50.fasta, 22,234 sequences) were translated, and the longest open reading frame was taken. CD-HIT was run as above, and a minimum length of 50 amino acids resulted in 20,884 sequences in the jgi90 data set. An in-house Perl script was run to split accidentally joined transcripts in both the wis90 and jgi90 sets, and the resulting transcripts were then combined in a final data set, together with the *D. bardawil* proteins from the NCBI, and CD-HIT at 90% was performed again. This resulted in the final data set of 83,694 sequences, called *D. salina/bardawil* proteome WIS.

General Annotation

Annotation was performed on the final protein data set with Blast2GO using the default parameters (Conesa et al., 2005). A total of 20,068 sequences were annotated.

Annotation of Mass Spectrometry Results

The mass spectrometry results were further annotated using Mercator (Lohse et al., 2014) and WebMGA (Kegg and Kog; Wu et al., 2011).

Specific Proteins/Protein Families

Proteins of interest were studied further. The sequences were analyzed with BLASTP at the NCBI (Altschul et al., 1997) to find similar proteins in other species. In extended protein families (ABC, PAP-fibrillin, acyl carrier, esterase, and lipase), members were first characterized in *D. bardawil*, and then those sequences were used to find orthologs in Arabidopsis (*Arabidopsis thaliana*), japonica rice (*Oryza sativa*), and *Chlamydomonas reinhardtii*. The Arabidopsis orthologs were found by BLASTP at The Arabidopsis Information Resource (www.arabidopsis.org; Lamesch et al., 2012), and the other species were found by using Arabidopsis as input into Greenphyl version 3 (http://www.greenphyl.org/cgi-bin/get_homologs.cgi; Rouard et al., 2011).

The sequences were then aligned with both ClustalW (version 2.1; Larkin et al., 2007) and Muscle (version 3.8.31; Edgar, 2004), and the better alignment was chosen for phylogenetic analysis. In cases where only one region was properly aligned, the alignment was cut manually into blocks (ABC1 and PAP-fibrillin). Phylogenetic analysis was performed with neighbor joining in ClustalW and ProML (Maximum Likelihood) in Phylip (version 3.69; Felsenstein, 2005).

Comparison with Other Data Sets

The core lipid droplet lists were compared with *C. reinhardtii* eyespot (Schmidt et al., 2006), two *C. reinhardtii* CLD (Moellering and Benning, 2010; Nguyen et al., 2011), one Arabidopsis plastoglobule (Lundquist et al., 2012b), and one chromoplast (Siddique et al., 2006) proteome collections using Proteinortho version 2.3 (Lechner et al., 2011). The best reciprocal BLAST hit for each collection compared with the βC-plastoglobuli or CLD was taken.

Supplemental Data

The following supplemental materials are available.

Supplemental Figure S1. CLD core proteome sequences list.

Supplemental Figure S2. βC-plastoglobuli core proteome sequences list.

Supplemental Figure S3. Metabolic diagram of βC-plastoglobuli and CGP metabolic pathways diagram showing identified enzymes in βC-plastoglobuli and CLD.

ACKNOWLEDGMENTS

We thank Dr. Irit Orr (Biological Service Unit at the Weizmann Institute) for help in preparing the proteome database and Dr. Alexandra Gabashvili (The Israel Center for Personalized Medicine Proteomics Unit) for help in the preparation of samples for proteomic analysis.

Received August 11, 2014; accepted November 11, 2014; published November 17, 2014.

LITERATURE CITED

Altschul SF, Madden TL, Schäffer AA, Zhang J, Zhang Z, Miller W, Lipman DJ (1997) Gapped BLAST and PSI-BLAST: a new generation of protein database search programs. Nucleic Acids Res **25:** 3389–3402

Barsan C, Sanchez-Bel P, Rombaldi C, Egea I, Rossignol M, Kuntz M, Zouine M, Latché A, Bouzayen M, Pech JC (2010) Characteristics of the tomato chromoplast revealed by proteomic analysis. J Exp Bot **61:** 2413–2431

Ben-Amotz A, Katz A, Avron M (1982) Accumulation of β-carotene in halotolerant algae: purification and characterization of β-carotene-rich globules from *Dunaliella bardawil*. J Phycol **18:** 529–537

Ben-Amotz A, Lers A, Avron M (1988) Stereoisomers of β-carotene and phytoene in the alga *Dunaliella bardawil*. Plant Physiol **86:** 1286–1291

Ben-Amotz A, Shaish A, Avron M (1989) Mode of action of the massively accumulated β-carotene of *Dunaliella bardawil* in protecting the alga against damage by excess irradiation. Plant Physiol **91:** 1040–1043

Besagni C, Kessler F (2013) A mechanism implicating plastoglobules in thylakoid disassembly during senescence and nitrogen starvation. Planta **237:** 463–470

Boyd JS, Mittelmeier TM, Lamb MR, Dieckmann CL (2011) Thioredoxin-family protein EYE2 and Ser/Thr kinase EYE3 play interdependent roles in eyespot assembly. Mol Biol Cell **22:** 1421–1429

Boyle NR, Page MD, Liu B, Blaby IK, Casero D, Kropat J, Cokus SJ, Hong-Hermesdorf A, Shaw J, Karpowicz SJ, et al (2012) Three acyltransferases and nitrogen-responsive regulator are implicated in nitrogen starvation-induced triacylglycerol accumulation in Chlamydomonas. J Biol Chem **287:** 15811–15825

Bréhélin C, Kessler F, van Wijk KJ (2007) Plastoglobules: versatile lipoprotein particles in plastids. Trends Plant Sci **12:** 260–266

Chapman ER (2008) How does synaptotagmin trigger neurotransmitter release? Annu Rev Biochem **77:** 615–641

Conesa A, Götz S, García-Gómez JM, Terol J, Talón M, Robles M (2005) Blast2GO: a universal tool for annotation, visualization and analysis in functional genomics research. Bioinformatics **21:** 3674–3676

Davidi L, Katz A, Pick U (2012) Characterization of major lipid droplet proteins from Dunaliella. Planta **236:** 19–33

Davidi L, Shimoni E, Khozin-Goldberg I, Zamir A, Pick U (2014) Origin of β-carotene-rich plastoglobuli in *Dunaliella bardawil*. Plant Physiol **164:** 2139–2156

Edgar RC (2004) MUSCLE: multiple sequence alignment with high accuracy and high throughput. Nucleic Acids Res **32:** 1792–1797

Eugeni Piller L, Glauser G, Kessler F, Besagni C (2014) Role of plastoglobules in metabolite repair in the tocopherol redox cycle. Front Plant Sci **5:** 298

Farese RV Jr, Walther TC (2009) Lipid droplets finally get a little R-E-S-P-E-C-T. Cell **139:** 855–860

Felsenstein J (2005) PHYLIP (Phylogeny Inference Package), Version 3.6. Department of Genome Sciences, University of Washington, Seattle

Finel M, Pick U, Selman-Reimer S, Selman BR (1984) Purification and characterization of a glycerol-resistant CF_0-CF_1 and CF_1-ATPase from the halotolerant alga *Dunaliella bardawil*. Plant Physiol **74:** 766–772

Giorio G, Stigliani AL, D'Ambrosio C (2007) Agronomic performance and transcriptional analysis of carotenoid biosynthesis in fruits of transgenic HighCaro and control tomato lines under field conditions. Transgenic Res **16:** 15–28

Goodman JM (2008) The gregarious lipid droplet. J Biol Chem **283:** 28005–28009

Grünewald K, Hirschberg J, Hagen C (2001) Ketocarotenoid biosynthesis outside of plastids in the unicellular green alga *Haematococcus pluvialis*. J Biol Chem **276:** 6023–6029

Horn PJ, James CN, Gidda SK, Kilaru A, Dyer JM, Mullen RT, Ohlrogge JB, Chapman KD (2013) Identification of a new class of lipid droplet-associated proteins in plants. Plant Physiol **162:** 1926–1936

Huang NL, Huang MD, Chen TL, Huang AH (2013) Oleosin of subcellular lipid droplets evolved in green algae. Plant Physiol **161:** 1862–1874

James GO, Hocart CH, Hillier W, Chen H, Kordbacheh F, Price GD, Djordjevic MA (2011) Fatty acid profiling of *Chlamydomonas reinhardtii* under nitrogen deprivation. Bioresour Technol **102:** 3343–3351

Jolivet P, Roux E, D'Andrea S, Davanture M, Negroni L, Zivy M, Chardot T (2004) Protein composition of oil bodies in *Arabidopsis thaliana* ecotype WS. Plant Physiol Biochem **42:** 501–509

Joyard J, Ferro M, Masselon C, Seigneurin-Berny D, Salvi D, Garin J, Rolland N (2009) Chloroplast proteomics and the compartmentation of plastidial isoprenoid biosynthetic pathways. Mol Plant **2:** 1154–1180

Katz A, Jimenez C, Pick U (1995) Isolation and characterization of a protein associated with carotene globules in the alga *Dunaliella bardawil*. Plant Physiol **108:** 1657–1664

Kreimer G (2009) The green algal eyespot apparatus: a primordial visual system and more? Curr Genet **55:** 19–43

Kroll D, Meierhoff K, Bechtold N, Kinoshita M, Westphal S, Vothknecht UC, Soll J, Westhoff P (2001) VIPP1, a nuclear gene of *Arabidopsis thaliana* essential for thylakoid membrane formation. Proc Natl Acad Sci USA **98:** 4238–4242

Lamesch P, Berardini TZ, Li D, Swarbreck D, Wilks C, Sasidharan R, Muller R, Dreher K, Alexander DL, Garcia-Hernandez M, et al (2012) The Arabidopsis Information Resource (TAIR): improved gene annotation and new tools. Nucleic Acids Res **40:** D1202–D1210

Larkin MA, Blackshields G, Brown NP, Chenna R, McGettigan PA, McWilliam H, Valentin F, Wallace IM, Wilm A, Lopez R, et al (2007) Clustal W and Clustal X version 2.0. Bioinformatics **23:** 2947–2948

Lechner M, Findeiss S, Steiner L, Marz M, Stadler PF, Prohaska SJ (2011) Proteinortho: detection of (co-)orthologs in large-scale analysis. BMC Bioinformatics **12:** 124

Lewis JD, Lazarowitz SG (2010) Arabidopsis synaptotagmin SYTA regulates endocytosis and virus movement protein cell-to-cell transport. Proc Natl Acad Sci USA **107:** 2491–2496

Li W, Godzik A (2006) Cd-hit: a fast program for clustering and comparing large sets of protein or nucleotide sequences. Bioinformatics **22:** 1658–1659

Lin IP, Jiang PL, Chen CS, Tzen JTC (2012) A unique caleosin serving as the major integral protein in oil bodies isolated from *Chlorella* sp. cells cultured with limited nitrogen. Plant Physiol Biochem **61:** 80–87

Lippold F, vom Dorp K, Abraham M, Hölzl G, Wewer V, Yilmaz JL, Lager I, Montandon C, Besagni C, Kessler F, et al (2012) Fatty acid phytyl ester synthesis in chloroplasts of *Arabidopsis*. Plant Cell **24:** 2001–2014

Lo SM, Theg SM (2012) Role of vesicle-inducing protein in plastids 1 in cpTat transport at the thylakoid. Plant J **71:** 656–668

Lohse M, Nagel A, Herter T, May P, Schroda M, Zrenner R, Tohge T, Fernie AR, Stitt M, Usadel B (2014) Mercator: a fast and simple web server for genome scale functional annotation of plant sequence data. Plant Cell Environ **37:** 1250–1258

Lundquist PK, Davis JI, van Wijk KJ (2012a) ABC1K atypical kinases in plants: filling the organellar kinase void. Trends Plant Sci **17:** 546–555

Lundquist PK, Poliakov A, Bhuiyan NH, Zybailov B, Sun Q, van Wijk KJ (2012b) The functional network of the Arabidopsis plastoglobule proteome based on quantitative proteomics and genome-wide coexpression analysis. Plant Physiol **158:** 1172–1192

Lundquist PK, Poliakov A, Giacomelli L, Friso G, Appel M, McQuinn RP, Krasnoff SB, Rowland E, Ponnala L, Sun Q, et al (2013) Loss of plastoglobule kinases ABC1K1 and ABC1K3 causes conditional degreening, modified prenyl-lipids, and recruitment of the jasmonic acid pathway. Plant Cell **25:** 1818–1839

Manara A, Dalcorso G, Leister D, Jahns P, Baldan B, Furini A (2013) AtSIA1 and AtOSA1: two Abc1 proteins involved in oxidative stress responses and iron distribution within chloroplasts. New Phytol **4:** 12533

Martinis J, Glauser G, Valimareanu S, Kessler F (2013) A chloroplast ABC1-like kinase regulates vitamin E metabolism in Arabidopsis. Plant Physiol **162:** 652–662

Mattjus P (2009) Glycolipid transfer proteins and membrane interaction. Biochim Biophys Acta **1788:** 267–272

Moellering ER, Benning C (2010) RNA interference silencing of a major lipid droplet protein affects lipid droplet size in *Chlamydomonas reinhardtii*. Eukaryot Cell **9:** 97–106

Murphy DJ (2012) The dynamic roles of intracellular lipid droplets: from archaea to mammals. Protoplasma **249:** 541–585

Nacir H, Bréhélin C (2013) When proteomics reveals unsuspected roles: the plastoglobule example. Front Plant Sci **4:** 114

Nguyen HM, Baudet M, Cuiné S, Adriano JM, Barthe D, Billon E, Bruley C, Beisson F, Peltier G, Ferro M, et al (2011) Proteomic profiling of oil bodies isolated from the unicellular green microalga *Chlamydomonas reinhardtii*: with focus on proteins involved in lipid metabolism. Proteomics **11:** 4266–4273

Nojima D, Yoshino T, Maeda Y, Tanaka M, Nemoto M, Tanaka T (2013) Proteomics analysis of oil body-associated proteins in the oleaginous diatom. J Proteome Res **12:** 5293–5301

Otters S, Braun P, Hubner J, Wanner G, Vothknecht UC, Chigri F (2013) The first α-helical domain of the vesicle-inducing protein in plastids 1 promotes oligomerization and lipid binding. Planta **237:** 529–540

Rosati C, Aquilani R, Dharmapuri S, Pallara P, Marusic C, Tavazza R, Bouvier F, Camara B, Giuliano G (2000) Metabolic engineering of beta-carotene and lycopene content in tomato fruit. Plant J **24:** 413–419

Rouard M, Guignon V, Aluome C, Laporte MA, Droc G, Walde C, Zmasek CM, Périn C, Conte MG (2011) GreenPhylDB v2.0: comparative and functional genomics in plants. Nucleic Acids Res **39:** D1095–D1102

Schapire AL, Valpuesta V, Botella MA (2009) Plasma membrane repair in plants. Trends Plant Sci **14:** 645–652

Schmidt M, Gessner G, Luff M, Heiland I, Wagner V, Kaminski M, Geimer S, Eitzinger N, Reissenweber T, Voytsekh O, et al (2006) Proteomic analysis of the eyespot of *Chlamydomonas reinhardtii* provides novel insights into its components and tactic movements. Plant Cell **18:** 1908–1930

Schulze T, Schreiber S, Iliev D, Boesger J, Trippens J, Kreimer G, Mittag M (2013) The heme-binding protein SOUL3 of *Chlamydomonas reinhardtii* influences size and position of the eyespot. Mol Plant **6:** 931–944

Siddique MA, Grossmann J, Gruissem W, Baginsky S (2006) Proteome analysis of bell pepper (*Capsicum annuum* L.) chromoplasts. Plant Cell Physiol **47:** 1663–1673

Silvestro D, Andersen TG, Schaller H, Jensen PE (2013) Plant sterol metabolism: Δ(7)-sterol-C5-desaturase (STE1/DWARF7), Δ(5,7)-sterol-Δ(7)-reductase (DWARF5) and Δ(24)-sterol-Δ(24)-reductase (DIMINUTO/DWARF1) show multiple subcellular localizations in *Arabidopsis thaliana* (Heynh) L. PLoS ONE **8:** e56429

Singh DK, McNellis TW (2011) Fibrillin protein function: the tip of the iceberg? Trends Plant Sci **16:** 432–441

Tenzer S, Moro A, Kuharev J, Francis AC, Vidalino L, Provenzani A, Macchi P (2013) Proteome-wide characterization of the RNA-binding protein RALY-interactome using the in vivo-biotinylation-pulldown-quant (iBioPQ) approach. J Proteome Res **12:** 2869–2884

Vieler A, Brubaker SB, Vick B, Benning C (2012) A lipid droplet protein of *Nannochloropsis* with functions partially analogous to plant oleosins. Plant Physiol **158:** 1562–1569

Vothknecht UC, Otters S, Hennig R, Schneider D (2012) Vipp1: a very important protein in plastids?! J Exp Bot **63:** 1699–1712

Wang ZT, Ullrich N, Joo S, Waffenschmidt S, Goodenough U (2009) Algal lipid bodies: stress induction, purification, and biochemical characterization in wild-type and starchless *Chlamydomonas reinhardtii*. Eukaryot Cell **8:** 1856–1868

Westphal S, Heins L, Soll J, Vothknecht UC (2001) Vipp1 deletion mutant of *Synechocystis*: a connection between bacterial phage shock and thylakoid biogenesis? Proc Natl Acad Sci USA **98:** 4243–4248

Wu S, Zhu Z, Fu L, Niu B, Li W (2011) WebMGA: a customizable web server for fast metagenomic sequence analysis. BMC Genomics **12:** 444

Ye X, Al-Babili S, Klöti A, Zhang J, Lucca P, Beyer P, Potrykus I (2000) Engineering the provitamin A (beta-carotene) biosynthetic pathway into (carotenoid-free) rice endosperm. Science **287:** 303–305

Youssef A, Laizet Y, Block MA, Maréchal E, Alcaraz JP, Larson TR, Pontier D, Gaffé J, Kuntz M (2010) Plant lipid-associated fibrillin proteins condition jasmonate production under photosynthetic stress. Plant J **61:** 436–445

Ytterberg AJ, Peltier JB, van Wijk KJ (2006) Protein profiling of plastoglobules in chloroplasts and chromoplasts: a surprising site for differential accumulation of metabolic enzymes. Plant Physiol **140:** 984–997

Zhang L, Sakamoto W (2013) Possible function of VIPP1 in thylakoids: protection but not formation? Plant Signal Behav **8:** e22860